5-2-2016

IFN-γ receptor and STAT1 signaling in B cells are central to spontaneous germinal center formation and autoimmunity.

Phillip P. Domeier
Pennsylvania State University College of Medicine

Sathi Babu Chodisetti
Pennsylvania State University College of Medicine

Chetna Soni
Pennsylvania State University College of Medicine

Stephanie L. Schell
Pennsylvania State University College of Medicine

Melinda J. Elias
Pennsylvania State University College of Medicine

See next page for additional authors

Let us know how access to this document benefits you

Follow this and additional works at: http://jdc.jefferson.edu/mifp

Part of the Medical Immunology Commons, and the Medical Microbiology Commons

Authors

Phillip P. Domeier, Sathi Babu Chodisetti, Chetna Soni, Stephanie L. Schell, Melinda J. Elias, Eric B. Wong, Timothy K. Cooper, Daisuke Kitamura, and Ziaur S.M. Rahman

JEM

IFN-γ receptor and STAT1 signaling in B cells are central to spontaneous germinal center formation and autoimmunity

Phillip P. Domeier,[1] Sathi Babu Chodisetti,[1]* Chetna Soni,[1]* Stephanie L. Schell,[1] Melinda J. Elias,[1] Eric B. Wong,[1] Timothy K. Cooper,[2,3] Daisuke Kitamura,[4] and Ziaur S.M. Rahman[1]

[1]Department of Microbiology and Immunology, [2]Department of Comparative Medicine, and [3]Department of Pathology, Pennsylvania State University College of Medicine, Hershey, PA 17033
[4]Research Institute for Biomedical Sciences, Tokyo University of Science, 162 0825 Tokyo, Japan

Spontaneously developed germinal centers (GCs [Spt-GCs]) harbor autoreactive B cells that generate somatically mutated and class-switched pathogenic autoantibodies (auto-Abs) to promote autoimmunity. However, the mechanisms that regulate Spt-GC development are not clear. In this study, we report that B cell–intrinsic IFN-γ receptor (IFN-γR) and STAT1 signaling are required for Spt-GC and follicular T helper cell (Tfh cell) development. We further demonstrate that IFN-γR and STAT1 signaling control Spt-GC and Tfh cell formation by driving T-bet expression and IFN-γ production by B cells. Global or B cell–specific IFN-γR deficiency in autoimmune B6.Sle1b mice leads to significantly reduced Spt-GC and Tfh cell responses, resulting in diminished antinuclear Ab reactivity and IgG$_{2c}$ and IgG$_{2b}$ auto-Ab titers compared with B6.Sle1b mice. Additionally, we observed that the proliferation and differentiation of DNA-reactive B cells into a GC B cell phenotype require B cell–intrinsic IFN-γR signaling, suggesting that IFN-γR signaling regulates GC B cell tolerance to nuclear self-antigens. The IFN-γR deficiency, however, does not affect GC, Tfh cell, or Ab responses against T cell–dependent foreign antigens, indicating that IFN-γR signaling regulates autoimmune, but not the foreign antigen–driven, GC and Tfh cell responses. Together, our data define a novel B cell–intrinsic IFN-γR signaling pathway specific to Spt-GC development and autoimmunity. This novel pathway can be targeted for future pharmacological intervention to treat systemic lupus erythematosus.

Germinal centers (GCs) are specialized microenvironments formed in the secondary lymphoid organs that generate high-affinity, long-lived antibody (Ab)-forming cells (AFCs) and memory B cells (Nutt and Tarlinton, 2011). GCs can spontaneously develop (spontaneously developed GCs [Spt-GCs]) without purposeful immunization or infection (Luzina et al., 2001; Cappione et al., 2005; Vinuesa et al., 2009; Wong et al., 2012; Hua et al., 2014; Jackson et al., 2014). We previously showed that in nonautoimmune B6 mice, Spt-GCs contribute to steady-state Ab production while maintaining B cell tolerance (Wong et al., 2012; Soni et al., 2014). Dysregulation of Spt-GC formation in human and mouse systemic lupus erythematosus (SLE) generates pathogenic antinuclear Ab (ANA)–specific IgG AFCs that lead to high titers of ANAs, the hallmark of SLE disease (Diamond et al., 1992; Cappione et al., 2005; Wellmann et al., 2005; Vinuesa et al., 2009; Tiller et al., 2010; Kim et al., 2011). Autoreactive B cells in Spt-GCs arise because of poor maintenance

of B cell tolerance at the GC checkpoint, a factor that is an integral component of SLE disease initiation (Vinuesa et al., 2009; Rahman, 2011). However, the pathway that promotes the aberrantly regulated Spt-GC response in SLE is not clear.

In human and mouse SLE, IFN-γ expression strongly correlates with disease severity (Pollard et al., 2013). IFN-γ deficiency or blockade reduces auto-Ab production and ameliorates renal disease in both MRL/MpJ-Fas^{lpr} and NZW/NZBF1 lupus mice (Jacob et al., 1987; Ozmen et al., 1995; Balomenos et al., 1998; Haas et al., 1998; Schwarting et al., 1998; Lawson et al., 2000), whereas excessive T cell–intrinsic IFN-γ signaling caused by decreased Ifng mRNA decay drives the accumulation of follicular T helper cells (Tfh cells) and subsequent Spt-GC and auto-Ab formation in mice homozygous for the san allele of Roquin (sanroque-Rc3h1^{san}; Lee et al., 2012). Increased production of IFN-γ has been reported in SLE patients (Csiszár et al., 2000; Harigai et al., 2008). Polymorphisms in the IFNG gene that drive increased IFN-γ expression are associated with SLE susceptibility (Kim et al., 2010). Also, blockade of IFN-γ has been shown to normalize IFN-regulated gene expression and serum CXCL10 in SLE patients (Welcher et al., 2015), highlighting the importance of IFN-γ receptor (IFN-γR) signaling in SLE de-

JEM

velopment. However, a B cell–intrinsic mechanism by which IFN-γ−IFN-γR signaling may drive Spt-GC development, leading to lupus-like autoimmunity, has not been described.

Lupus-prone B6.*Sle1b* mice develop larger and poorly regulated Spt-GCs as a result of altered B cell selection at the GC tolerance checkpoint (Wong et al., 2012, 2015). This altered GC checkpoint is driven by lupus-associated signaling lymphocyte activation molecule family genes (Wandstrat et al., 2004; Wong et al., 2015). Correspondingly, B6.*Sle1b* female mice exhibit significantly higher numbers of Spt-GC B cells and Tfh cells that promote elevated ANA titers (Wong et al., 2012, 2015). Consistent with other lupus models (Walsh et al., 2012; Hua et al., 2014; Jackson et al., 2014; Soni et al., 2014), we recently reported a B cell–intrinsic requirement for TLR7 and MyD88 signaling in Spt-GC development and subsequent autoimmunity in B6.*Sle1b* mice (Soni et al., 2014). The B cell–intrinsic mechanism by which IFN-γR signaling may promote Spt-GC development in B6.*Sle1b* mice or other autoimmune-prone mice is unknown.

In this study, we first used the B6 model of Spt-GC formation to study the role and mechanisms by which IFN-γR and STAT1 signaling may control the Spt-GC response without the confounding effects of any autoimmune susceptibility genes. We found that B cell–intrinsic IFN-γR expression is essential for Spt-GC development, indicating that IFN-γ signaling serves as a novel GC initiation or maintenance factor. The reduction in Spt-GC response in B6.IFN-γR$_1^{-/-}$ mice correlated with a decrease in IgG-producing AFCs and lower IgG, IgG$_{2b}$, and IgG$_{2c}$ Ab titers compared with B6 control mice. We performed a thorough analysis of B cell–intrinsic mechanisms of IFN-γR and STAT1 signaling that control Spt-GC formation. We found that IFN-γR signaling in B cells controls Spt-GC and Tfh cell development through STAT1-mediated and T-bet–dependent IFN-γ production by B cells. Subsequently, we determined how IFN-γR signaling might contribute to Spt-GC and Tfh cell responses in autoimmune-prone B6.*Sle1b* mice, leading to autoimmunity. Similar to the results obtained in the B6 model, we found significantly reduced Spt-GC and Tfh cell responses in B6.*Sle1b*.IFN-γR$_1^{-/-}$ mice and in BM chimeric mice in which B6.*Sle1b* B cells lacked IFN-γR. The reduction in Spt-GC responses in both of these mice led to diminished ANA reactivity and significantly lower ANA-specific IgG AFCs and ANA titers than in B6.*Sle1b* mice. Finally, using an adoptive B cell transfer system, we showed a defect in proliferation and differentiation of DNA-reactive B cells into a GC phenotype in the absence of IFN-γR signaling in B cells. Together, our data delineate a previously unappreciated B cell–intrinsic mechanism of IFN-γ signaling in driving Spt-GC development and autoimmunity.

RESULTS
IFN-γ–IFN-γR signaling is essential for Spt-GC B cell and Tfh cell development
Given the role of IFN-γ signaling in promoting IgG Ab production (Pollard et al., 2013), we asked whether IFN-γ signaling is involved in Spt-GC development. We found that B6 mice deficient in IFN-γR$_1$ (B6.IFN-γR$_1^{-/-}$) had significantly reduced percentages of B220$^+$PNA^{hi}Fas^{hi} GC B cells and CD4$^+$PD1^{hi}CXCR5^{hi} Tfh cells than wild-type B6 mice (Fig. 1, A and B). Immunohistochemical labeling of IgD$^-$PNA$^+$ GC B cells revealed an absence of Spt-GC formation in the spleens of B6.IFN-γR$_1^{-/-}$ mice (Fig. 1 C). Additionally, the B220$^+$ B cell population in B6.IFN-γR$_1^{-/-}$ mice showed significantly reduced expression of the activation marker CD86 (Fig. 1 D). B6.IFN-γR$_1^{-/-}$ mice also had a significantly lower number of IgG-producing AFCs than wild-type B6 mice, but IgM-producing AFCs were not significantly different between the two groups (Fig. 1, E and F). Similar results were seen in IFN-γ–deficient B6 mice (not depicted). The reduction in Spt-GC and IgG AFC responses translated to decreased levels of total IgG (Fig. 1 G), IgG$_{2b}$ (Fig. 1 I), and IgG$_{2c}$ (Fig. 1 J) in sera from B6.IFN-γR$_1^{-/-}$ mice compared with control B6 mice. No significant differences were observed in IgG$_1$ (Fig. 1 H) or IgM (Fig. 1 K) serum titers. Together, these data indicate that IFN-γR signaling is required for Spt-GC development and for the production of IgG$_{2b}$ and IgG$_{2c}$ Abs.

IFN-γR deficiency does not alter primary B cell development or foreign antigen–induced GC (iGC), Tfh cell, or Ab responses
Next, we evaluated whether the absence of Spt-GCs and significantly reduced IgG$_{2b}$ and IgG$_{2c}$ Ab titers in B6.IFN-γR$_1^{-/-}$ mice could be attributed to global defects in primary B cell development and/or the ability of B cells to mount an immune response. To determine whether the lack of IFN-γR expression altered BM B cell development, we analyzed subpopulations of the early B cell progenitors and found no significant difference in fractions A–F (Hardy et al., 1991) between the two groups (Fig. 2, A and B). We also did not observe any significant differences in peripheral immature B cells, including transitional type 1, type 2, and type 3 as well as mature B cell populations, including follicular and marginal zone B cells in the spleen (Fig. 2, C and D; Allman et al., 2001). B6.IFN-γR1$^{-/-}$ mice did not show an alteration in surface expression of B cell maturation markers IgD, MHCII, IgM, or CD23 compared with B6 control mice (Fig. 2, E–H).

To study whether IFN-γR signaling is involved in foreign antigen iGC, Tfh cell, and AFC responses, we evaluated the B cell immune response against the T cell–dependent antigen NP-CGG (4-hydroxy-3-nitrophenylacetyl–conjugated chicken γ-globulin) 14 d after immunization. We observed not a lower but rather a higher proportion of NP-specific GC B cells in B6.IFN-γR1$^{-/-}$ mice than B6 control mice (Fig. 3 A). We also observed no differences in NP-specific IgG and IgG$_1$ AFCs (Fig. 3, C and D) nor anti–NP IgG and IgG$_1$ Ab responses (Fig. 3, E and F) between B6 and B6.IFN-γR1$^{-/-}$ mice. The percentage of Tfh cells in B6 mice was also not different from B6.IFN-γR1$^{-/-}$ mice (Fig. 3 B). Together, these data indicate that IFN-γR signaling is not involved in the foreign antigen–driven GC, Tfh cell, and AFC responses nor primary B cell development.
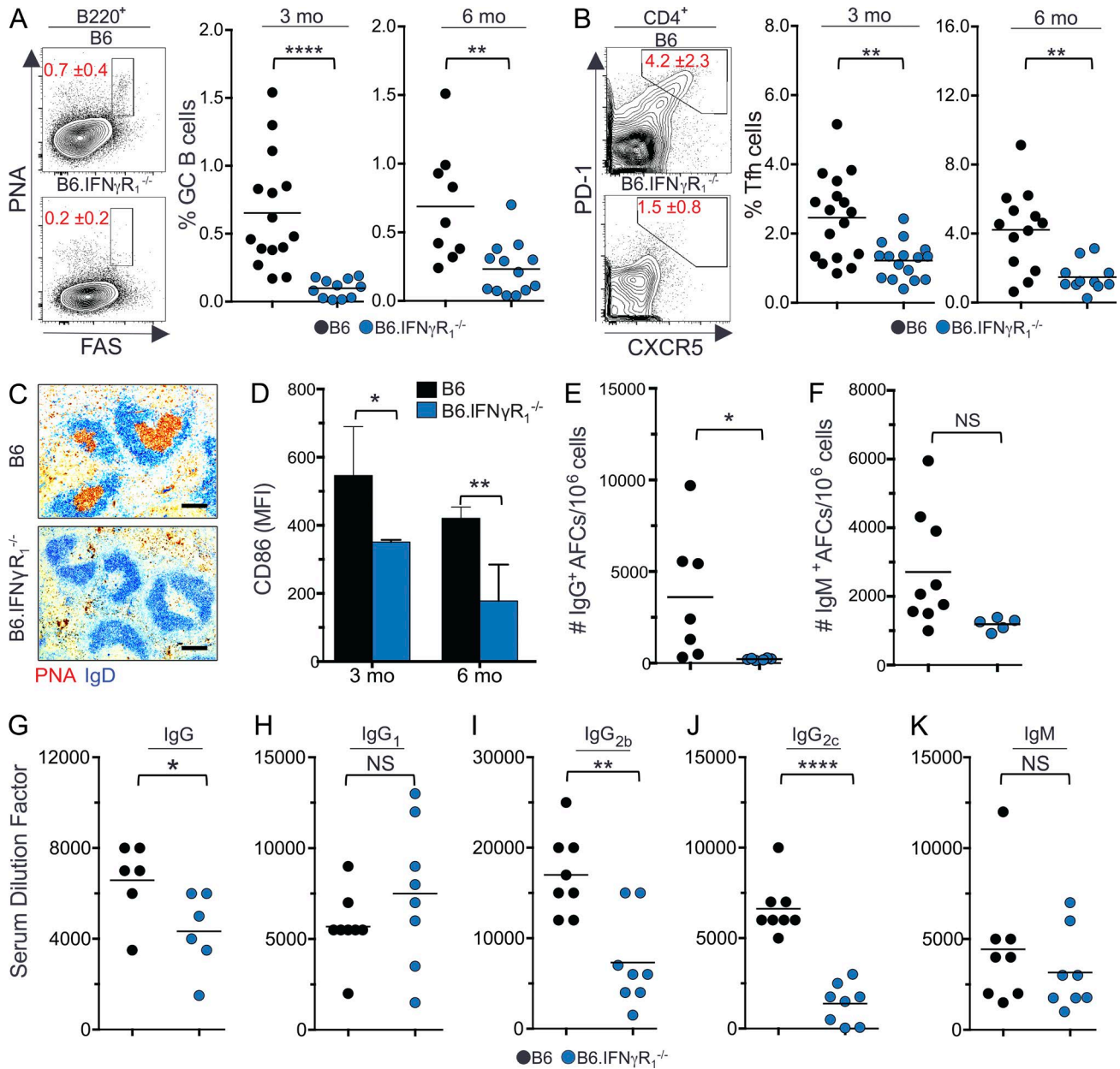
Figure 1. **IFN–γR signaling is required for Spt-GC formation and IgG production.** (A and B) The percentages of B220+Fas^hiPNA^hi GC B cells (A) and CD4+CXCR5^hiPD-1^hi Tfh cells (B) were obtained from flow cytometric analysis of spleen cells of 3- and 6-mo-old B6 and B6.IFN-γR$_1$$^{-/-}$ mice. Each symbol represents a mouse (*n* = 11–15). (C) Representative histological images of spleen sections from 6-mo-old mice (*n* = 5 per group) stained with the GC B cell marker PNA and anti-IgD. Bars, 150 µm. (D) Flow cytometric analysis of CD86 expression (MFI) on total B220+ B cells at 3 and 6 mo of age (*n* = 5 mice per group). Error bars are mean ± SD. (E and F) Numbers of IgG+ (E) and IgM+ (F) splenic AFCs in 6-mo-old mice of indicated strains (*n* = 5–9). (G–K) Analysis of serum titers of IgG, IgG$_1$, IgG$_{2b}$, IgG$_{2c}$, and IgM Abs in 6-mo-old mice by ELISA. Each symbol represents a mouse (*n* = 6–8). The data shown are the cumulative results of two or three independent experiments. Statistical values were determined using an unpaired, nonparametric, Mann–Whitney Student's *t* test. Horizontal lines indicate mean values. *, P < 0.05; **, P < 0.01; ****, P < 0.001.

IFN–γR signaling drives Spt-GC development in a B cell–intrinsic manner

To determine whether the requirement of IFN–γR signaling in the formation of Spt-GCs is B cell intrinsic, we first compared IFN–γR expression between B cells and T cells and found that IFN–γR surface expression was higher in B cells than in T cells (Fig. 4 A), with IFN–γR expression being significantly higher in B220+PNA^hiFas^hi Spt-GC B cells than in B220+ non-GC B cells (Fig. 4 A). In contrast, IFN–γR expression on Tfh cells was significantly lower than naive T cells and B cells (not depicted).

JEM

A B220$^+$CD43$^+$

B6   B6.IFNγR$_1$

B B220$^+$CD43$^-$

B6   B6.IFNγR$_1^{-/-}$

C B220$^+$CD93$^+$

B6   B6.IFNγR$_1^{-/-}$

D B220$^+$CD93$^-$

B6   B6.IFNγR$_1^{-/-}$

●B6
○B6.IFNγR$_1^{-/-}$

●B6
○B6.IFNγR$_1^{-/-}$

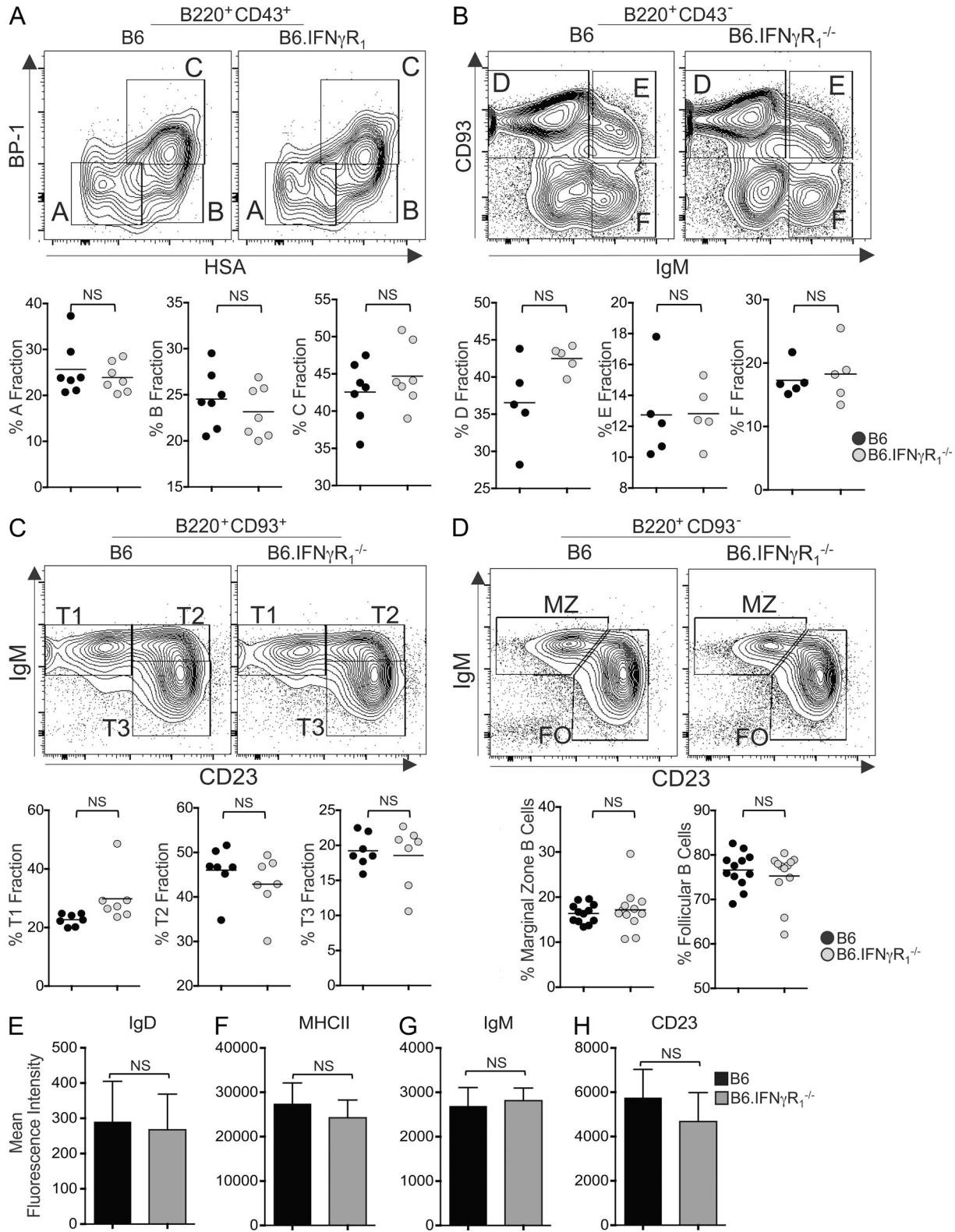**E** IgD   **F** MHCII   **G** IgM   **H** CD23

■B6
■B6.IFNγR$_1^{-/-}$

Figure 2. IFN–γR signaling in B cell development. (A) Flow cytometric analysis of isolated BM populations for B cell developmental fractions A (B220$^+$CD43$^+$HSA$^-$BP-1$^-$), B (B220$^+$CD43$^+$HSA$^+$BP-1$^-$), and C (B220$^+$CD43$^+$HSA$^+$BP-1$^+$). HSA, heat-stable antigen. (B) Flow cytometric analysis of isolated BM populations for B cell developmental fractions D (B220$^+$CD43$^-$IgM$^-$CD93$^+$), E (B220$^+$CD43$^-$IgM$^+$CD93$^+$), and F (B220$^+$CD43$^-$IgM$^+$CD93$^-$) with plotted values for each fraction shown. (C) Flow cytometric analysis of isolated splenocyte populations for B cell developmental stages T1 (B220$^+$AA4.1$^+$CD23$^-$IgM$^+$), T2

Next, combinations of mature naive B cells and T cells were transferred from B6 or B6.IFN-$\gamma R_1^{-/-}$ mice into $Rag_1^{-/-}$ mice (Fig. 4, B and C). $Rag_1^{-/-}$ mice that received IFN-γR–deficient B cells and B6 T cells failed to develop Spt-GCs as evaluated by histology (Fig. 4, B and C, second column). These mice also had significantly reduced numbers of IgG$^+$ AFCs compared with B6 B cell and B6 T cell combinations as controls (not depicted). In contrast, Spt-GCs were formed in $Rag_1^{-/-}$ mice that received IFN-γR–deficient T cells and B6 B cells (Fig. 4, B and C, third column), highlighting the importance of IFN-γR expression on B cells in Spt-GC development. To confirm the B cell–intrinsic role of IFN-γR signaling in Spt-GC formation, we generated mixed BM chimeras by reconstituting lethally irradiated B6.μMT mice, which lack mature B cells, with a mixture of BM cells (80% derived from B6.μMT mice and 20% derived from either B6 or B6.IFN-$\gamma R_1^{-/-}$ mice). BM-reconstituted mice were rested for 3 mo before analysis. Mice reconstituted with IFN-γR–deficient BM cells exhibited significantly reduced percentages of B220$^+$ PNA^{hi}Fas^{hi} GC B cells and CD4$^+$PD1^{hi}CXCR5^{hi} Tfh cells than mice reconstituted with B6 BM cells as measured by flow cytometry (Fig. 4, D and E). Consistent with the flow cytometry data, spleens from recipients of IFN-γR–deficient BM cells exhibited a significantly reduced number and size of IgD$^-$GL7$^+$ Spt-GCs (Fig. 4 F). These data demonstrate that IFN-γR expression on B cells is required for Spt-GC development.

IFN–γ–mediated T-bet expression and IFN–γ production by B cells are critical for Spt-GC development

Previous studies have identified the role of T-bet in IFN-γ–mediated IgG$_{2a}$ class switching (Peng et al., 2002; Xu and Zhang, 2005; Rubtsova et al., 2013). We therefore asked whether T-bet was involved in the development of Spt-GCs. We first examined T-bet expression in B cells and found that T-bet RNA (Fig. 5 A) and protein (Fig. 5 B) expression were significantly higher in Spt-GC B cells than in non-GC B cells and foreign antigen (NP-OVA) iGC B cells. No significant difference was observed between non-GC and iGC B cell T-bet expression (Fig. 5, A and B). The increased T-bet expression in Spt-GC B cells was associated with increased IFN-γ production by these cells compared with non-GC B cells (Fig. 5, C and D). During Spt-GC development, IFN-γ expression in vivo was significantly higher in pre-Tfh cells than naive T cells (Fig. 5 E). However, IFN-γ expression was down-regulated in GC Tfh cells to levels similar to naive T cells (Fig. 5 E). Spt-GC and iGC B cells exhibited similar levels of Bcl-6 expression (not depicted).

To ask whether IFN-γ signaling drives T-bet expression and IFN-γ production by GC B cells, we used a 40LB fibroblast–based culture system (Nojima et al., 2011) to induce GC B cells ex vivo (see Materials and methods section In vitro GC B cell development assay). When these ex vivo–generated GC B cells were cultured further for 4 d, their GC B cell phenotype could be maintained in the presence of either IL-4 or IFN-γ (Fig. 5 F). Treatment of these GC B cells with IFN-γ increased T-bet expression (Fig. 5, G and H) and IFN-γ production (Fig. 5 I), highlighting the role of T-bet and IFN-γ in maintaining the in vitro GC B cell phenotype. T-bet was not induced in and IFN-γ was not produced by these GC B cells in the presence of IL-4 (Fig. 5, G–I).

Finally, to evaluate the role of T-bet in Spt-GC formation in vivo, we analyzed T-bet–deficient B6 (B6.T-bet$^{-/-}$) mice. B6.T-bet$^{-/-}$ mice had significantly reduced Spt-GC and Tfh cell responses than B6 mice at 3 mo of age (Fig. 6, A and B). Immunohistochemical labeling of IgD$^-$GL7$^+$ GC B cells revealed a significantly reduced size of Spt-GCs in the spleens of B6.T-bet$^{-/-}$ mice compared with B6 mice (Fig. 6 C). T-bet deficiency also strongly correlated with reduced IgG, IgG$_{2b}$, and IgG$_{2c}$ serum Ab titers in B6.T-bet$^{-/-}$ mice (Fig. 6, D–F). By treating ex vivo–generated GC B cells from B6.T-bet$^{-/-}$ mice with IFN-γ, we further observed that the maintenance of the GC B cell phenotype (Fig. 6 G) and IFN-γ production by GC B cells (Fig. 6 H) were dependent on T-bet expression and IFN-γ production by these cells. Altogether, our data highlight the significance of T-bet expression and IFN-γ production by B cells in driving Spt-GC development.

IFN-γR–mediated Spt-GC formation is STAT1 dependent

To determine mechanistically how IFN-γR signaling in B cells controls Spt-GC formation, we measured pSTAT1 (pY701) and pSTAT3 (pY705) levels in B cells and found that B220$^+$PNA^{hi}Fas^{hi} Spt-GC B cells had increased levels of STAT1, pSTAT1, and pSTAT3 compared with B220$^+$ non-GC B cells (Fig. 7 A). Several studies using T cells have described STAT1-independent expression of T-bet and production of IFN-γ (Ramana et al., 2002; Johnson and Scott, 2007). Activation of both STAT1 and STAT3 by IFN-γ signaling in acute myeloid leukemia cells was also previously reported (Sato et al., 1997). Therefore, we first determined whether IFN-γR signaling in B cells drove only STAT1 or both STAT1 and STAT3 phosphorylation. We treated purified naive B cells with IFN-γ in vitro and found a significant increase in pSTAT1 (Fig. 7 B) but not pSTAT3 (Fig. 7 C) within 5–15 min of IFN-γ treatment. By treating B cells with IFN-γ alone, anti-IgM alone, or IFN-γ plus anti-IgM, we

---

(B220$^+$AA4.1$^+$CD23$^+$IgM$^+$), and T3 (B220$^+$AA4.1$^+$CD23$^-$IgM$^-$) with plotted values for each fraction shown. (D) Flow cytometric analysis of isolated splenocyte populations for marginal zone (MZ) B cells (B220$^+$CD93$^-$CD23$^-$IgM$^+$) and mature B cells (B220$^+$CD93$^-$CD23$^+$IgM$^+$) with plotted values for each fraction shown. Each symbol represents a mouse (n = 5–7). FO, follicular. (E–H) Plotted mean fluorescence intensity values show expression of IgD, MHCII, IgM, and CD23 on total splenic B220$^+$ cells. Error bars are mean ± SD (n = 5 mice per group). Data represent two to three independent experiments. Statistical values were determined using an unpaired, nonparametric, Mann–Whitney Student's t test.
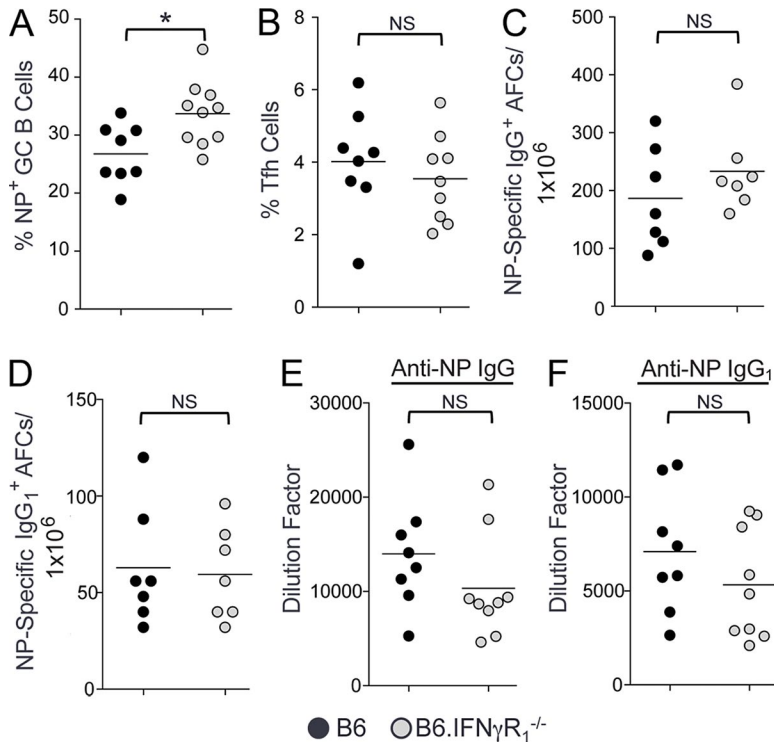
Figure 3. **IFN-γR deficiency does not alter foreign antigen iGC, Tfh cell, or AFC responses.** (A and B) B6 (black circles) and B6.IFN-γR₁⁻/⁻ (gray circles) mice were immunized with NP-CGG. Flow cytometric analysis was performed on splenocytes 14 d after immunization to obtain the percentages of B220⁺FasʰⁱPNAʰⁱ NP-specific GC B cells (A) and CD4⁺CXCR5ʰⁱPD-1ʰⁱ Tfh cells (B). (C and D) Quantification of NP-specific IgG⁺ (C) and IgG₁⁺ (D) AFCs by ELISPOT assay in splenocytes obtained from these mice 14 d after immunization. (E and F) Anti-NP IgG (E) and IgG₁ (F) Ab titers are measured in sera obtained from mice described in A–D. These data represent seven to nine mice per group for all panels. Data are the cumulative results of two independent experiments. Statistical values were determined using an unpaired, nonparametric, Mann–Whitney Student's *t* test. *, P < 0.05.

further observed that the IFN-γ–induced STAT1 phosphorylation in naive B cells was independent of B cell receptor (BCR) stimulation (Fig. 7 D).

Finally, to study the role of STAT1 in Spt-GC development, we analyzed B6 mice deficient in STAT1 (B6.STAT1⁻/⁻) for Spt-GC formation at 6 mo of age. B6.STAT1⁻/⁻ mice had significantly reduced percentages of Spt-GC B cells and Tfh cells (Fig. 7 E) and had no Spt-GC formation in the spleen compared with B6 control mice (Fig. 7 F). To further study a B cell–intrinsic requirement of STAT1 in Spt-GC development, we conditionally deleted STAT1 in B cells by crossing B6.STAT1ᶠˡᵒˣ/ᶠˡᵒˣ mice with CD19ᶜʳᵉ mice (CD19ᶜʳᵉSTAT1ᶠˡ/ᶠˡ). We found significantly lower GC and Tfh cell responses in CD19ᶜʳᵉSTAT1ᶠˡ/ᶠˡ mice than in B6.STAT1ᶠˡᵒˣ/ᶠˡᵒˣ control mice (Fig. 7 G). Our histological analysis showed a lack of Spt-GC formation in CD19ᶜʳᵉSTAT1ᶠˡ/ᶠˡ mice and well-formed GCs in B6.STAT1ᶠˡ/ᶠˡ control mice (Fig. 7 H), highlighting the significance of B cell–intrinsic IFN-γR and STAT1 signaling in Spt-GC development. By treating ex vivo–generated STAT1-deficient GC B cells with IFN-γ, we observed that the maintenance of the GC B cell phenotype (Fig. 7 I), T-bet expression (Fig. 7 J), and IFN-γ mRNA expression (Fig. 7 K) by GC B cells were dependent on STAT1.

The critical B cell–intrinsic role of IFN-γR signaling in IFN-γR–mediated Spt-GC and auto-Ab responses
IFN-γR signaling is implicated in ANA production and Ab-mediated pathology in SLE disease (Pollard et al., 2013). Spt-GCs are likely a major source of autoreactive B cells, leading to auto-Ab production and the development of auto-

immunity (Diamond et al., 1992; Cappione et al., 2005; Wellmann et al., 2005; Vinuesa et al., 2009; Tiller et al., 2010; Kim et al., 2011). To determine the role of IFN-γR signaling in the elevated Spt-GC response in SLE-prone mice, we crossed B6.IFN-γR₁⁻/⁻ mice to autoimmune-prone B6.Sle1b mice (named B6.Sle1b.IFN-γR₁⁻/⁻). B6.Sle1b mice carry lupus-associated polymorphic signaling lymphocyte activation molecule family genes (Wandstrat et al., 2004). Correspondingly, B6.Sle1b female mice exhibit an increased number of ANA-producing AFCs and high serum titers of ANAs as a result of significantly higher numbers of Spt-GC B cells and Tfh cells than wild-type B6 mice (Wong et al., 2012, 2015). We found that B6.Sle1b.IFN-γR₁⁻/⁻ mice had a significantly reduced percentage of B220⁺PNAʰⁱFasʰⁱ GC B cells and CD4⁺PD1ʰⁱCXCR5ʰⁱ Tfh cells compared with B6.Sle1b control mice (Fig. 8, A and B). The reduction of Spt-GC response in B6.Sle1b.IFN-γR₁⁻/⁻ mice was confirmed by immunohistochemical analysis, which revealed significantly smaller and fewer IgD⁻GL7⁺ GC structures in B6.Sle1b.IFN-γR₁⁻/⁻ spleens compared with B6.Sle1b controls (Fig. 8 C). The number of splenic IgG⁺ and IgM⁺ AFCs was significantly reduced in B6.Sle1b.IFN-γR₁⁻/⁻ mice compared with B6.Sle1b controls (Fig. 8 D). A decrease in the number of long-lived IgM⁺ and IgG⁺ AFCs was observed in the BM of B6.Sle1b.IFN-γR₁⁻/⁻ mice compared with B6.Sle1b mice (Fig. 8 E). We also generated mixed BM chimeras by reconstituting lethally irradiated B6.μMT mice with a mixture of BM cells (80% derived from B6.μMT mice and 20% derived from either B6.Sle1b or B6.Sle1b.IFN-γR₁⁻/⁻ mice). Mice reconstituted with BM cells from B6.Sle1b.IFN-γR₁⁻/⁻ mice
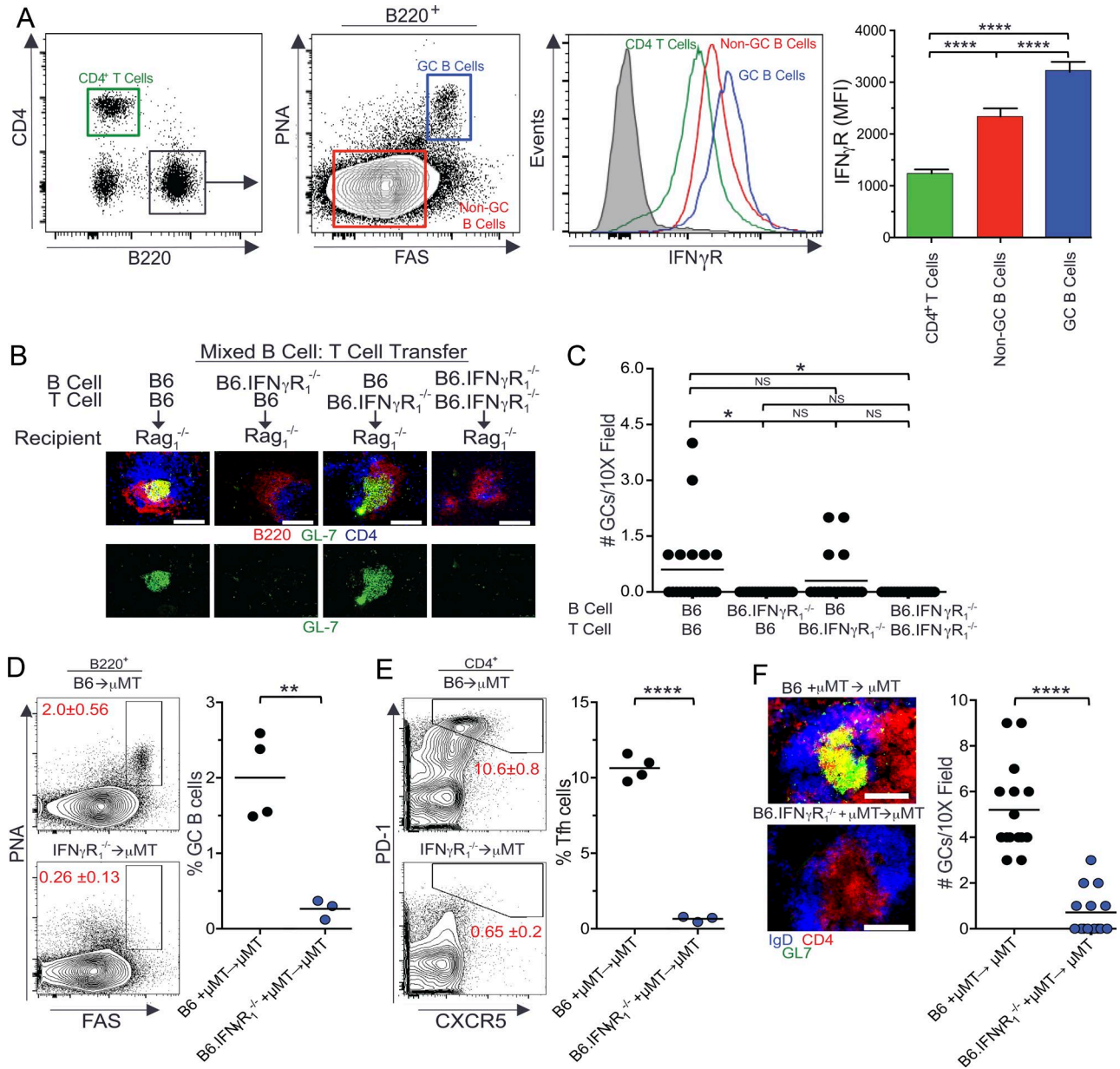
Figure 4. **B cell–intrinsic requirement of IFN-γR signaling in Spt-GC and Tfh cell development.** (A) Flow cytometric analysis of surface expression of IFN-γR on CD4+ T cells, B220+PNA−Fas− non-GC B cells, and B220+PNAhiFashi GC B cells. The mean IFN-γR surface expression (mean fluorescence intensity ± SD) in these three cell types from five mice of each genotype is shown in the right panel. Filled gray histogram indicates isotype control. (B) Representative images of spleen sections from Rag1−/− mice (five mice per group) that received combinations of naive B and T cells are shown. Sections were stained with anti-B220, anti-CD4, and GC B cell marker GL-7. Bottom panels show only GC B cell staining with GL-7. (C) Quantification of the number of GCs observed per 10× field from similar spleen sections shown in B (n = 5 mice per group). (D and E) The percentages of B220+FashiPNAhi GC B cells (D) and CD4+CXCR5hiPD-1hi Tfh cells (E) were obtained from flow cytometric analysis of spleen cells of 3-mo-old μMT mice reconstituted with BM cells from B6 and B6.IFN-γR1−/− mice. Each symbol represents a mouse (n = 3-4 mice per group). (F) Representative images of spleen sections from μMT mice (3–4 mice per group) described in D and E are shown (left) in which sections were stained with GL-7, anti-IgD, and anti-CD4. The number of GCs observed per 10× field from these mice (n = 3–4) is shown in the right panel. These data are representative of two independent experiments. In C, statistical analysis was performed by one-way ANOVA with a follow-up Tukey multiple-comparison test. In A, B, and D–F, statistical values were determined using an unpaired, nonparametric, Mann–Whitney Student's t test. *, P < 0.05; **, P < 0.01; ****, P < 0.001. Bars,150 μm.
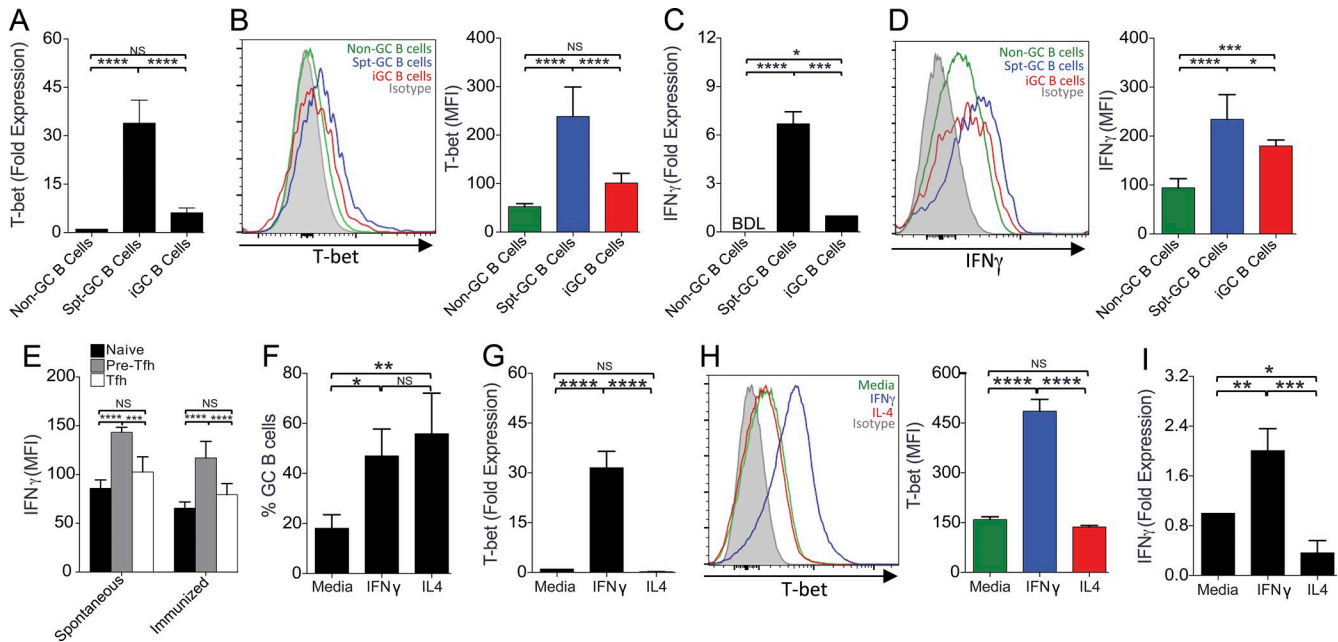
Figure 5. **Elevated T-bet expression and IFN-γ production by spontaneous GC B cells and IFN-γ–treated GC B cells.** (A) Quantitative RT-PCR analysis of T-bet transcripts in B220⁺PNA⁻Fas⁻ non-GC B cells, B220⁺PNAʰⁱFasʰⁱ Spt-GC B cells, and B220⁺PNAʰⁱFasʰⁱ iGC B cells analyzed at 14 d after NP-OVA immunization. (B) Flow cytometric analysis of intracellular T-bet expression (by mean fluorescence intensity) in non-GC B cells, Spt-GC B cells, and iGC B cells. (C) Quantitative RT-PCR analysis of IFN-γ transcripts. BDL, below detectable level. (D) Flow cytometric analysis of intracellular IFN-γ production (by MFI) in non-GC B cells, Spt-GC B cells, and iGC B cells. (E) Flow cytometric analysis of intracellular IFN-γ levels in naive T cells (CD4⁺PD-1ˡᵒCXCR5ˡᵒ), pre-Tfh cells (CD4⁺PD-1ⁱⁿᵗCXCR5ⁱⁿᵗ), and Tfh cells (CD4⁺PD-1ʰⁱCXCR5ʰⁱ) during Spt-GC and iGC responses. (F) Maintenance of ex vivo–generated GC B cell phenotype in the presence of IFN-γ or IL-4. (G) Quantitative RT-PCR analysis of T-bet transcripts in GC B cells described in F. (H) Flow cytometric analysis of intracellular T-bet expression in GC B cells described in F. (I) Quantitative RT-PCR analysis of IFN-γ transcripts in GC B cells described in F. In all panels, data are representative of three replicate experiments with at least three mice per group. Statistical analysis was performed by one-way ANOVA with a follow-up Tukey multiple-comparison test. Error bars are mean ± SD. *, P < 0.05; **, P < 0.01; ***, P < 0.001; ****, P < 0.0001.

exhibited significantly reduced percentages of GC B cells (Fig. 8 F, left) and Tfh cells (Fig. 8, right) than mice reconstituted with B6.*Sle1b* BM cells. Consistent with the flow cytometry data, spleens from recipients of IFN-γR–deficient B6.*Sle1b* BM cells exhibited a significantly reduced number and size of IgD⁻GL7⁺ Spt-GCs (Fig. 8 G). Together, these data suggest the B cell–intrinsic role of IFN-γR signaling in the dysregulated Spt-GC and Tfh cell responses in B6.*Sle1b* mice, leading to the accumulation of auto-Abs.

To determine the B cell–intrinsic role of IFN-γR signaling in driving the proliferation and differentiation of autoreactive B cells into GCs, we used a well-characterized adoptive transfer system that involves the transfer of p-azophenyl arsonate (Ars) and DNA dual-reactive heavy chain knock in (named HKIR) B cells into syngeneic CD45.1/CD45.2 recipients preimmunized with Ars–keyhole limpet hemocyanin 1 wk before B cell transfer (Rahman et al., 2007; Vuyyuru et al., 2009; Wong et al., 2012). We performed a competition assay in which a mixture of Cell Trace–labeled 2 × 10⁵ CD45.1⁺ HKIR B cells and 2 × 10⁵ CD45.2⁺ HKIR B cells deficient in IFN-γR₁ (HKIR.IFN-γR₁⁻/⁻) were transferred i.v. into Ars–keyhole limpet hemocyanin–immunized B6.CD45.1/45.2 recipients. 4 d after cell transfer, we ana-

lyzed HKIR B cell proliferation and GC B cell differentiation into the GC phenotype. On average, 20% of transferred HKIR B cells actively proliferated as measured by Cell Trace dye dilution (Fig. 8 H). Notably, the proliferation of transferred HKIR.IFN-γR₁⁻/⁻ B cells was significantly lower than competing HKIR B cells in the same recipients (Fig. 8 H, right). In addition, a greater percentage of HKIR B cells differentiated into GC B cells (B220⁺PNAʰⁱFasʰⁱ) compared with HKIR.IFN-γR₁⁻/⁻ B cells (Fig. 8 I).

IFN-γR signaling promotes ANA development through the Spt–GC pathway in B6.*Sle1b* mice

Given the role of IFN-γR signaling in driving ANA-specific HKIR B cell proliferation and differentiation into the GC B cell phenotype (Fig. 8, H and I), we asked whether decreased Spt-GC and Tfh cell responses in B6.*Sle1b*.IFN-γR₁⁻/⁻ mice resulted in reduced ANA reactivity in these mice. Compared with B6.*Sle1b* control mice, we found that B6.*Sle1b*.IFN-γR₁⁻/⁻ mice had significantly lower numbers of double-stranded DNA (dsDNA)–, histone-, and nucleosome-specific AFCs in both spleen (Fig. 9 A) and BM cells (long-lived AFCs; Fig. 9 B). Consistent with the AFC data, we observed a significant decrease in serum ANA positivity in B6.*Sle1b*.
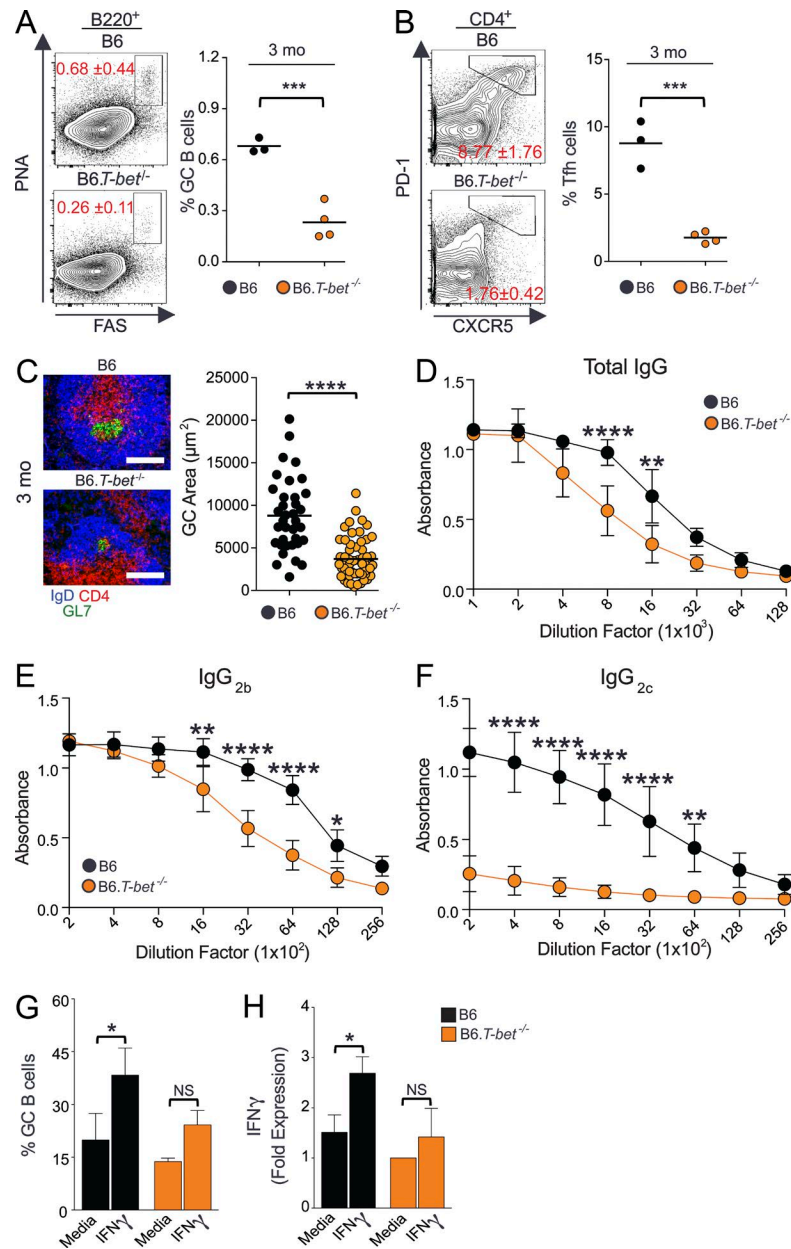
722

IFN-γR signaling controls spontaneous GC formation | Domeier et al.

Figure 6. **Critical role of T–bet in Spt–GC development and Th1 Ab responses.** (A and B) Percentages of B220^{+} Fas^{hi}PNA^{hi} GC B cells (A) and CD4^{+}CXCR5^{hi}PD-1^{hi} Tfh cells (B) obtained from flow cytometric analysis of spleen cells of 3-mo-old B6 and B6.*T-bet^{-/-}* mice. Each symbol represents a mouse (*n* = 3–4). (C) Representative images of spleen sections from 3-mo-old B6 and B6.*T-bet^{-/-}* mice stained with GL7, anti-CD4, and anti-IgD. GC area measurement is shown in the right panel (*n* = 3–4 mice per group). Bars, 150 μm. (D–F) Total serum Ab titers of IgG (D), IgG$_{2b}$ (E), and IgG$_{2c}$ (F) measured by ELISA (*n* = 3–4 per group). (G) Maintenance of ex vivo–generated GC B cell phenotype of B6 and B6.*T-bet^{-/-}* mice in media alone or with IFN-γ. (H) Quantitative RT-PCR analysis of IFN-γ transcripts in ex vivo–generated GC B cells (as described in G) from B6 and B6.*T-bet^{-/-}* mice (*n* = 3–4 mice per group). The data shown in G and H are representative of three independent experiments. In D–F, statistical analysis was performed by one-way ANOVA with a follow-up Tukey multiple-comparison test. In A–C, G, and H, statistical values were determined using an unpaired, nonparametric, Mann–Whitney Student's *t* test. Error bars are mean ± SD. *, $P < 0.05$; **, $P < 0.01$; ***, $P < 0.001$; ****, $P < 0.001$.

IFN-γR$_1^{-/-}$ mice compared with B6.*Sle1b* mice as indicated by the fluorescence intensity of the nuclear staining on HEp-2 slides (Fig. 9 C). In addition, we observed a decrease in nuclear antigen–specific seropositivity in B6.*Sle1b*.IFN-γR$_1^{-/-}$ mice compared with B6.*Sle1b* mice (Fig. 9 C). To confirm the findings of the ANA positivity measured by Hep-2 assay and to measure isotype- and subclass-specific serum ANA titers, we performed ELISA for specific nuclear antigens. B6.*Sle1b*.IFN-γR$_1^{-/-}$ mice had a significant reduction in serum titers of IgG$_{2b}$ and IgG$_{2c}$ Abs specific for nucleosome, histone, and dsDNA than B6.*Sle1b* controls (Fig. 9, D–F). Reduced auto-Ab titers in B6.*Sle1b*.IFN-γR$_1^{-/-}$ mice correlated with a reduced glomerular nephritis score (Fig. 9 G). We also observed a significantly reduced number

of total IgG AFCs (Fig. 9 H) as well as histone- and dsDNA–specific AFCs (Fig. 9, I and J) in chimeric mice in which B6.*Sle1b* B cells lacked IFN-γR compared with chimeric mice that received B6.*Sle1b* BM cells. Consistent with the AFC data, we found diminished ANA reactivity in μMT mice receiving B6.*Sle1b*. IFN-γR1$^{-/-}$ BM cells compared with B6.*Sle1b* control mice (Fig. 9 K). Together, these results suggest the B cell–intrinsic role of IFN-γR signaling in Spt-GC development and subsequent auto-Ab production, leading to kidney pathology in B6.*Sle1b* mice.

DISCUSSION

B cells play a central role in SLE disease pathogenesis (Sanz, 2014; Jackson et al., 2015). Therefore, understanding the
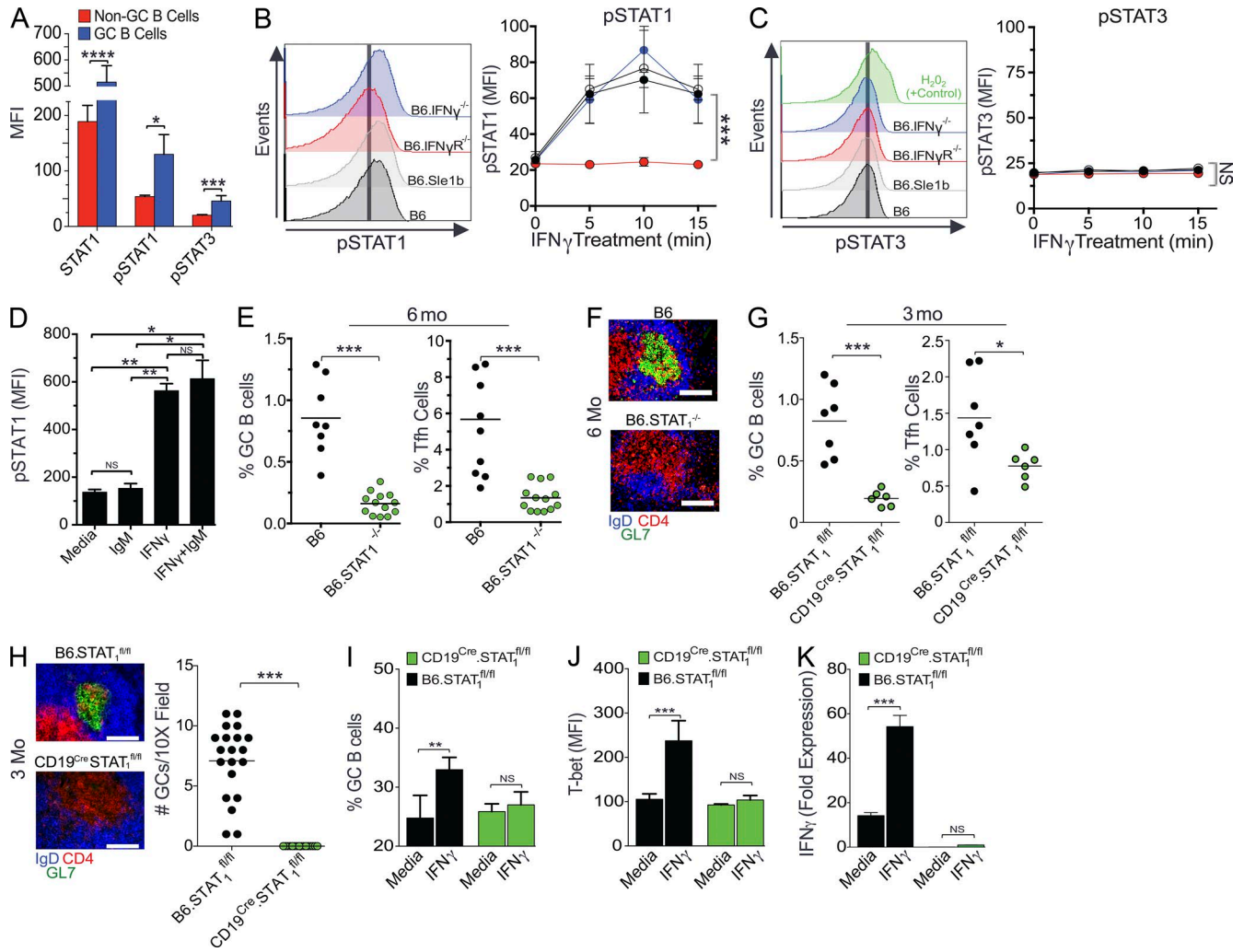
Figure 7. **B cell–intrinsic IFN–γR stimulus drives GC differentiation through STAT1, but not STAT3, phosphorylation.** (A) Flow cytometric analysis of intracellular STAT1, pSTAT1, and pSTAT3 expression (by mean fluorescence intensity) in B220[+]PNA[−]Fas[−] non-GC B cells and B220[+]PNA[hi]Fas[hi] GC B cells. These data represent five mice per group in three replicate experiments. (B and C) Flow cytometric analysis of intracellular pSTAT1 (B) and pSTAT3 (C) expression (mean fluorescence intensity) in B220^{+} cells after treatment of purified B cells with IFN-γ in vitro for the indicated time points. These data represent five mice per group in three replicate experiments. (D) Flow cytometric analysis of intracellular pSTAT1 expression (MFI) in B220^{+} cells with and without treatment of B cells with IgM alone, IFN-γ alone, or both IgM and IFN-γ in vitro for 10 min. These data represent five mice per group in three replicate experiments. (E) Flow cytometric analysis of percentages of B220^{+}Fas^{hi}PNA^{hi} GC B cells and CD4^{+}CXCR5^{hi}PD-1^{hi} Tfh cells in 6-mo-old mice. (F) Representative histological images of spleen sections from 6-mo-old B6 and B6.STAT1^{−/−} mice (five mice per group) stained with the GC B cell marker GL7, anti-CD4, and anti-IgD. (G) Flow cytometric analysis of the percentages of GC B cells and Tfh cells. (H) Representative histological images and quantification of GC structures of spleen sections from 3-mo-old B6.STAT1^{fl/fl} and CD19[Cre/+]STAT1^{fl/fl} mice (six mice per group). (I) Maintenance of ex vivo–generated GC B cell phenotype of B cells obtained from B6.STAT1^{fl/fl} and CD19[Cre/+]STAT1^{fl/fl} mice in the presence of IFN-γ. (J) Flow cytometric analysis of intracellular T-bet expression in GC B cells described in H. (K) Quantitative RT-PCR analysis of IFN-γ transcripts in GC B cells treated with IFN-γ as described in H. For H–J, n = 3 per group in three replicate experiments. In B and C, statistical analysis was performed by one-way ANOVA with a follow-up Tukey multiple-comparison test. Otherwise, statistical values were determined using an unpaired, nonparametric, Mann–Whitney Student's *t* test. Error bars are mean ± SD. *, P < 0.05; **, P < 0.01; ***, P < 0.001. Bars: (F) 150 µm; (H) 75 µm.

mechanisms that drive autoreactive B cell development would help specifically target these cells in treating SLE patients. Given the recently appreciated positive association of IFN-γ in SLE pathogenesis, in the current study, we determined the B cell–intrinsic role of IFN-γR signaling in promoting Spt-GC development and autoimmunity. Although it is not

clear what triggers the development of Spt-GCs, our published data indicate that both nonautoimmune B6 mice and autoimmune-prone B6.*Sle1b* mice develop Spt-GCs (Wong et al., 2012, 2015; Soni et al., 2014). We believe that the factor that triggers Spt-GC formation in B6 mice is identical to that observed in B6.*Sle1b* mice and is the basis for the dysregu-
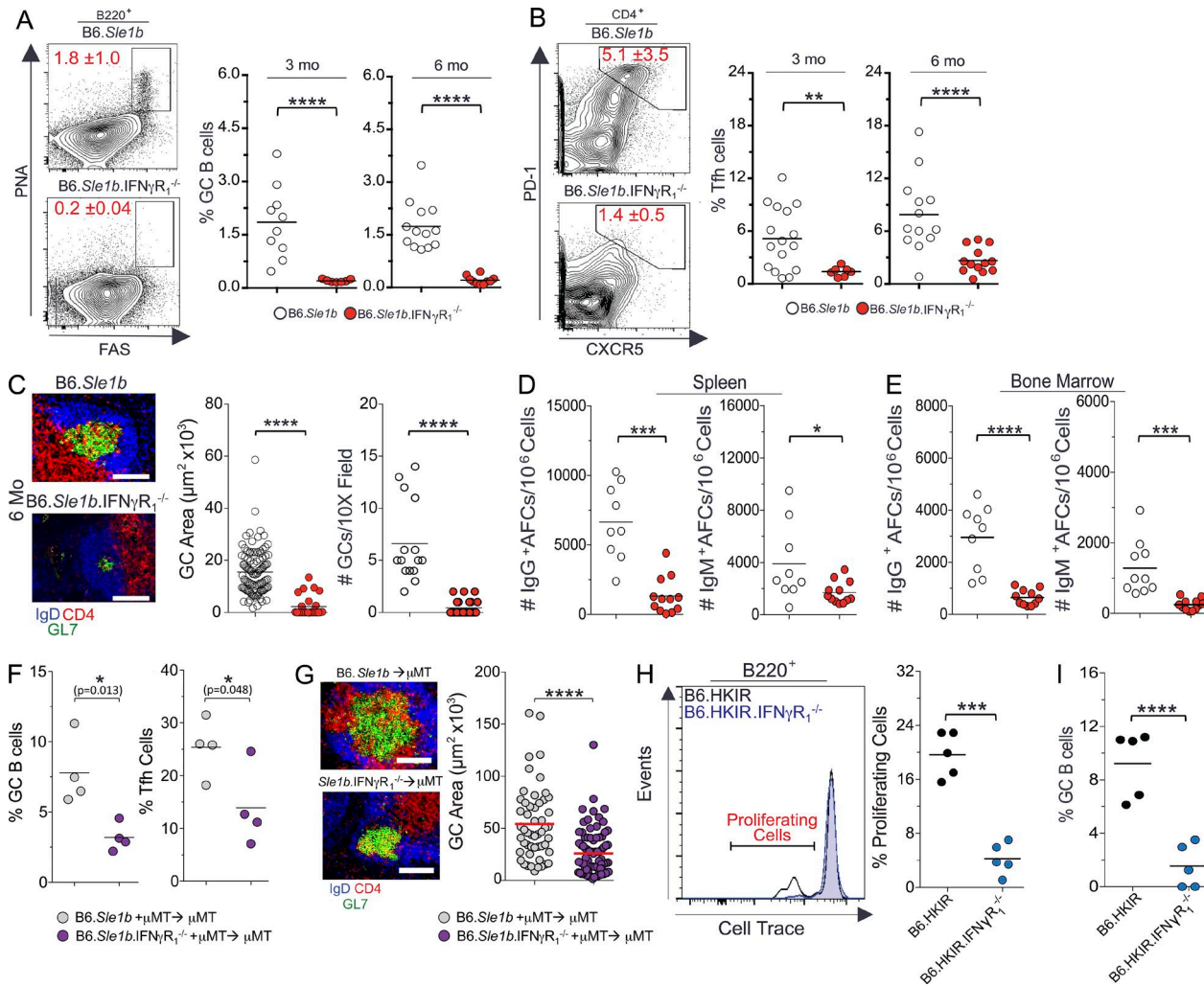
Figure 8. Reduced Spt-GC responses in global or B cell–specific IFN-γR–deficient autoimmune B6.*Sle1b* **mice.** (A and B) Percentages of B220+ FashiPNAhi GC B cells (A) and CD4+CXCR5hiPD-1hi Tfh cells (B) were obtained from flow cytometric analysis of spleen cells of 3- and 6-mo-old B6.*Sle1b* (*n* = 10) and B6.*Sle1b*.IFN-γR$_1$$^{-/-}$ mice (*n* = 10). (C) Representative images of spleen sections from 6-mo-old mice (five mice per group) stained with GL7, anti-CD4, and anti-IgD. GC area measurement (middle) and the quantification of the number of GCs per 10× field (right) are shown. (D) Quantification of IgG+ (left) and IgM+ (right) splenic AFCs in 6-mo-old mice (*n* = 10 mice per group). (E) Quantification of IgG+ (left) and IgM+ (right) BM AFCs in 6-mo-old mice (*n* = 9 mice per group). (F) The percentages of B220+FashiPNAhi GC B cells (left) and CD4+CXCR5hiPD-1hi Tfh cells (right) were obtained from flow cytometric analysis of spleen cells from 3-mo-old B6.μMT mice reconstituted with BM cells from B6.*Sle1b* and B6.*Sle1b*.IFN-γR$_1$$^{-/-}$ mice (four mice per group). (G) Representative images of spleen sections from μMT mice (four mice per group) described in F are shown (left) in which sections were stained with GL-7, anti-IgD, and anti-CD4. The GC areas (randomly chosen 10 GCs per mouse) from the spleens of mice described in F are shown in the right panel. (H and I) Percentages of B6.HKIR and B6.HKIR.IFN-γR$_1$$^{-/-}$ B cells undergoing proliferation (H) and GC B cell differentiation (I) in recipient mice. Where applicable, each symbol represents a mouse (*n* = 5 mice per group). The data shown are representative of three independent experiments. Statistical values were determined using an unpaired, nonparametric, Mann–Whitney Student's *t* test. Error bars are mean ± SD. *, P < 0.05; **, P < 0.01; ***, P < 0.001; ****, P < 0.001. Bars, 150 μm.

lated Spt-GC response caused by autoimmune susceptibility genes in B6.*Sle1b* mice and other lupus mice. Therefore, we first determined the B cell–specific role of IFN-γR signaling in Spt-GC formation and Tfh cell development without the confounding effects of any autoimmune susceptibility genes by using the B6 model. We further demonstrated that IFN-γR and STAT1 signaling drive Spt-GC development through the expression of T-bet and the production of IFN-γ by B cells. Subsequently, we showed the B cell–intrinsic role

of IFN-γR signaling in Spt-GC and Tfh cell responses in autoimmune-prone B6.*Sle1b* mice, leading to autoimmunity.

Spt-GCs can form in response to endogenous or self-antigens. In SLE-prone mice and SLE patients, altered regulation in the Spt-GC and Tfh cell responses helps generate somatically mutated pathogenic auto-Abs (Diamond et al., 1992; Cappione et al., 2005; Wellmann et al., 2005; Vinuesa et al., 2009; Tiller et al., 2010; Kim et al., 2011). We have previously shown that B cell–intrinsic, but not T cell-intrinsic,

Figure 9.   **B6.Sle1b.IFN–γR$_1$$^{-/-}$ mice exhibit reduced ANA titers and ANA–specific AFCs.** (A and B) Quantification of dsDNA- (left), histone- (middle), and nucleosome- (right) specific AFCs in total splenocytes (A) and in BM cells (B) from indicated mouse strains (n = 7–10 mice per group). (C) ANA detection by fluorescent HEp-2 assay using sera from 6-mo-old mice (n = 5 mice per group). Representative images from five mice of each genotype are shown. Fluorescence intensity (gray values) of staining (right) and pie charts summarize the distribution of serum samples exhibiting nonreactivity (non–HEp-2
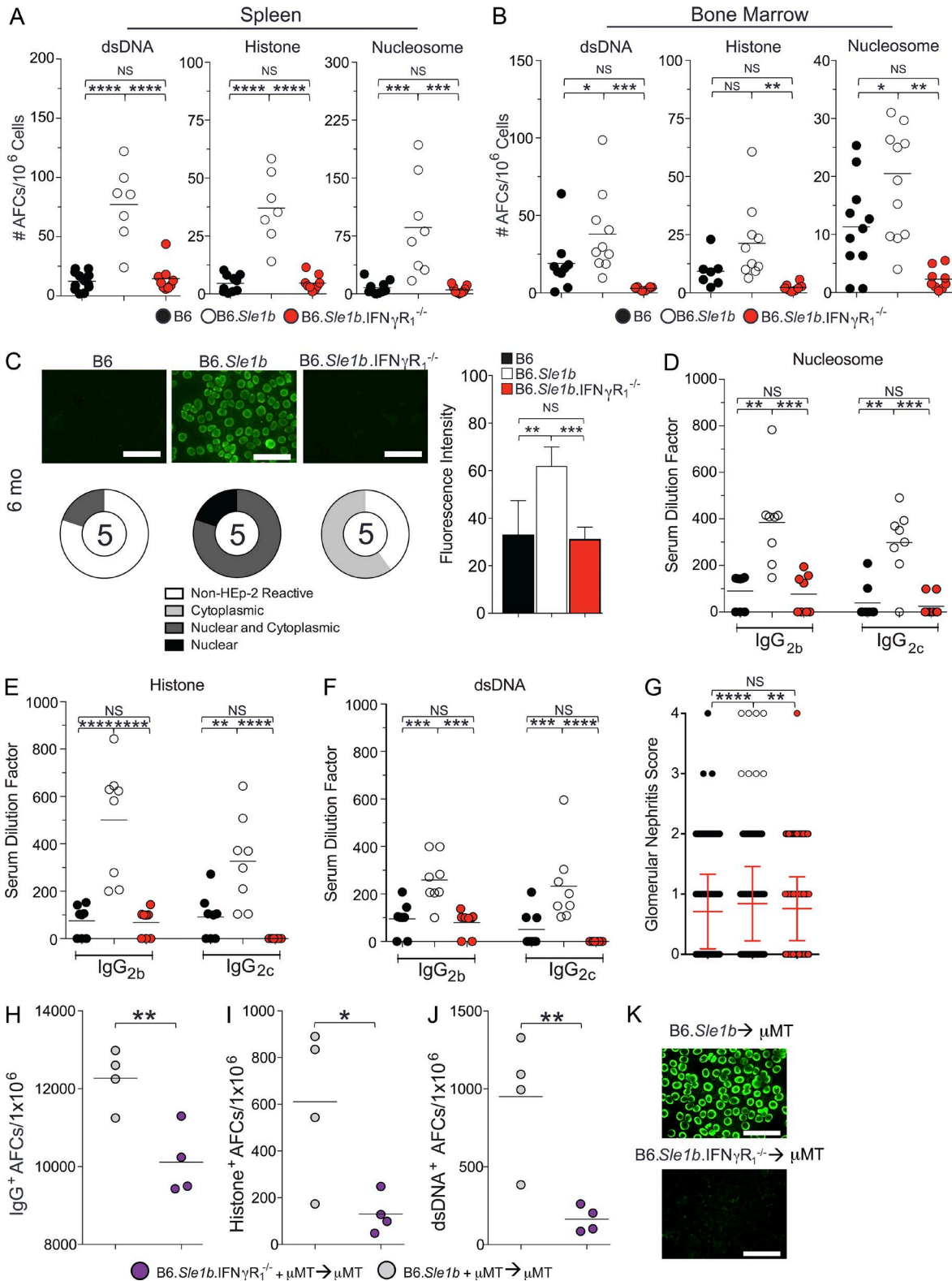
726

IFN–γR signaling controls spontaneous GC formation | Domeier et al.

expression of the lupus susceptibility locus *Sle1b* leads to elevated Spt-GC, Tfh cell, and auto-Ab responses in B6.*Sle1b* mice (Wong et al., 2012). Mutations in the Wiskott-Aldrich syndrome (*Was*) gene, a disease-associated allelic variant of protein tyrosine phosphatase nonreceptor 22 (*Ptpn22*) and *Lyn* deficiency, have also been shown to promote Spt-GC, Tfh cell, and autoimmune responses in a B cell–intrinsic manner (Dai et al., 2013; Hua et al., 2014; Jackson et al., 2014). Alternatively, Lee et al. (2012) have reported that dysregulated Spt-GC and autoimmune responses in sanroque mice result from an accumulation of Tfh cells in a T cell–intrinsic manner. Using the sanroque lupus model, Lee et al. (2012) showed that excessive IFN-γ production by T cells and T cell–intrinsic IFN-γ signaling profoundly increases Tfh cell accumulation and subsequent elevation of Spt-GC and auto-Ab responses. In this model, B cell–intrinsic IFN-γR deficiency did not significantly affect the Spt-GC, Tfh cell, and auto-Ab responses. However, we find a B cell–intrinsic requirement of IFN-γR signaling in the formation of Spt-GCs and Tfh cells. This differential B cell– and T cell–intrinsic role of IFN-γR signaling in Spt-GCs, Tfh cells, and autoimmunity may be attributed to two different models with distinct mechanisms for the loss of B cell tolerance, leading to SLE disease pathogenesis.

Using the B6.*Sle1b* model, we recently reported a B cell–intrinsic requirement of TLR7 in the formation of Spt-GCs and class-switched auto-Abs (Soni et al., 2014). Other groups have confirmed the essential role of TLR7 in promoting Spt-GC, Tfh cell, and auto-Ab responses (Walsh et al., 2012; Hua et al., 2014; Jackson et al., 2014). Based on the role of BCR and TLR dual receptor signaling in autoimmune B cell activation (Leadbetter et al., 2002; Viglianti et al., 2003), synergistic BCR and TLR7 signaling are likely promoting Spt-GC, Tfh cell, and auto-Ab responses in lupus-prone mice. Interestingly, the absence of IFN-γR and STAT1 signaling also abrogates the development of well-formed Spt-GCs and auto-Ab generation in B6.*Sle1b* mice. The deficiency of TLR7 or IFN-γR signaling, however, does not significantly affect the GC, Tfh cell, or Ab responses against T cell–dependent foreign antigens. Together, these data indicate that TLR7 and IFN-γR signaling in the development of Spt-GCs and autoimmunity are mechanistically distinct from foreign antigen–driven GC (iGC) and Tfh cell responses.

IL-21 secreted by GC Tfh cells is the major cytokine that controls GC and Tfh cell responses (Tellier and Nutt, 2013). Previous studies showed a B cell–intrinsic role of IL-21 signaling in regulating GC and Ab responses elicited by protein immunization (Linterman et al., 2010; Zotos et al., 2010). Spt-GC responses were also significantly reduced in IL-21R–deficient MRL/MpJ-*Fas^lpr* mice (Rankin et al., 2012). Recently, Bessa et al. (2010) described the B cell–intrinsic role of IL-21 and TLR (TLR7/8) signaling in the GC and Ab responses against virus-like particles loaded with bacterial RNA. We and other groups recently showed a B cell–intrinsic requirement of TLR7 and MyD88 signaling in the Spt-GC and Tfh cell responses (Walsh et al., 2012; Hua et al., 2014; Jackson et al., 2014; Soni et al., 2014). TLR stimulation has been shown to be associated with increased IFN-γ production in T cells and myeloid cells (Chalifour et al., 2004; Caron et al., 2005). Our published data on the role of TLR7 (Soni et al., 2014) and current findings about the role of IFN-γR signaling in the Spt-GC, Tfh cell, and auto-Ab responses in B6.*Sle1b* mice suggest that IFN-γR signaling may function downstream of TLR7 signaling, as TLR7 signaling can drive T-bet expression (Berland et al., 2006) and IFN-γ production in B cells. Although further studies are required to definitively determine the role of IFN-γR and IL-21R signaling at different stages of Spt-GC development, our data suggest that IFN-γR signaling in B cells is important in initiating Spt-GC formation.

Although the role of STAT1 and STAT3 signaling in B cell activation has recently been described in both mouse and human studies (Su et al., 1999; Xu and Zhang, 2005; Fornek et al., 2006; Avery et al., 2010), the role of STAT1 and/or STAT3 in IFN-γR–mediated Spt-GC development is not clear. We observed higher levels of pSTAT1 and pSTAT3 in Spt-GC B cells than non-GC B cells. By treating B cells ex vivo with IFN-γ, we showed only phosphorylation of STAT1 and not of STAT3. These data indicate that STAT3 phosphorylation is driven by a different pathway, such as by IL-21R, IL-6R, and IFN-αR signaling. Interestingly, we show an absolute requirement of B cell–intrinsic STAT1 expression for Spt-GC development, indicating that STAT1 may be required for initiating the Spt-GC formation. STAT1 was previously shown to be required for IgG auto-Ab production and B cell expression of TLR7 in pristane-induced lupus mice (Thibault et al., 2008). STAT1 expression in MRL/MpJ-*Fas^lpr* mice was also associated with increased kidney nephritis and SLE-like disease (Dong et al., 2007). Recently, a lupus risk variant that

reactive), reactivity to cytoplasmic antigens (cytoplasmic), reactivity to nuclear and cytoplasmic antigens (nuclear and cytoplasmic), and reactive to nuclear antigens only (nuclear). The numbers in the centers of the graphs denote the number of samples analyzed per group (bottom left). (D–F) Analysis of serum IgG$_{2b}$ and IgG$_{2c}$ Ab titers specific to nucleosome, histone, or dsDNA. Each symbol represents an individual mouse (n = 8–10 mice per group). (G) PAS-stained kidney sections of 6-mo-old female mice of each genotype (n = 5 mice per group) were analyzed for glomerular pathology. At least 100 glomeruli per mouse were individually scored for mesangioproliferative changes by a pathologist who was blinded to the sample genotypes. Error bars show mean ± SD. PAS, periodic acid–Schiff. (H–J) The numbers of IgG- (H), histone- (I), and ds-DNA– (J) specific AFCs in 3-mo-old B6.μMT mice reconstituted with BM cells from B6.*Sle1b* and B6.*Sle1b*.IFN-γR$_1$$^{-/-}$ mice (four mice per group). (K) Detection of ANA reactivity by fluorescent HEp-2 assay in mice described in H–J. The data shown are representative of two or three independent experiments. In A–G, statistical analysis was performed by one-way ANOVA, with a follow-up Tukey multiple-comparison test. In H–K, statistical values were determined using an unpaired, nonparametric, Mann–Whitney Student's t test. *, $P < 0.05$; **, $P < 0.01$; ***, $P < 0.001$; ****, $P < 0.001$. Bars, 75 μm.

is associated with decreased ETS1 and a high incidence of SLE has been shown to have increased pSTAT1 binding to DNA near the risk variant, spanning *ETS1* gene in B cells (Lu et al., 2015). These data suggest that B cell–intrinsic IFN-γR and STAT1 signaling are crucial for Spt-GC development and autoreactive B cell selection in the GCs.

A combination of BCR, TLR7, and IFN-γR signaling has been proposed to drive T-bet expression, which was shown to drive the expression of a recently described age-associated B cell phenotype and class switching to IgG$_{2a}$ and IgG$_{2c}$ Abs (Rubtsov et al., 2013; Rubtsova et al., 2013, 2015). TLR7 signaling in RNA-specific 564Igi B cells has also been shown to drive T-bet expression and production of IgG$_{2a}$ and IgG$_{2c}$ Abs (Berland et al., 2006). How a synergy in BCR, TLR7, and IFN-γR signaling and T-bet expression in B cells may shape the Spt-GC response has not been described. In this study, we found that T-bet expression is significantly higher in Spt-GC B cells, which is, in turn, required for IFN-γ and IgG$_{2c}$ Ab production. By analyzing T-bet–deficient mice, we further showed that T-bet is critical for Spt-GC development. Although Spt-GC B cells and age-associated B cells share some common properties (i.e., increased expression of *Fas* and low expression of IgD), their lineage relationship remains to be defined. It will be interesting to determine whether one population serves as a precursor for the other population or whether they are two distinct B cell lineages with different functions.

Previous in vitro studies by Lund and co-workers have identified the molecular mechanisms that regulate IFN-γ production by B effector 1 (Be1) cells (Harris et al., 2005). IFN-γ production by Be1 cells is dependent on expression of the IFN-γR and the T-box transcription factor T-bet. Lund and co-workers also identified Be1 cells in mice infected with pathogens (i.e., *Toxoplasma gondii* or *Heligmosomoides polygyrus*), which preferentially induce a type 1 immune response (Harris et al., 2000). Differentiation of Be1 lineage cells into the GC B cell phenotype during spontaneous activation of B cells under nonautoimmune or autoimmune conditions has not been investigated. By performing mature B cell and T cell cotransfer as well as BM chimeric experiments, we discovered that IFN-γR expression on B cells is critical for Spt-GC and Tfh cell development. Compared with non-GC and iGC B cells, we observed higher T-bet expression in and IFN-γ production by Spt-GC B cells. We further demonstrated that treatment of in vitro–generated GC B cells with IFN-γ drives T-bet expression, which promotes IFN-γ production by GC B cells. Collectively, these data suggest a potential differentiation of Be1 lineage cells into the Spt-GC B cell phenotype during spontaneous immune responses against endogenous ligand or self-antigen, which requires IFN-γR signaling, T-bet expression, and IFN-γ production by B cells.

In summary, we show that IFN-γR signaling in B cells and B cell IFN-γ production are the critical initial steps for Spt-GC development leading to autoimmunity. IFN-γR signaling controls Spt-GC formation by phosphorylating STAT1 and up-regulating T-bet in B cells, which is required for Spt-GC formation, IFN-γ production, and class switching to IgG$_{2b}$ and IgG$_{2c}$ Abs. Given our data on the B cell–intrinsic requirement of STAT1 in Spt-GC and Tfh cell development, we propose that in addition to its role in initiating Spt-GC formation by up-regulating T-bet expression and IFN-γ production, STAT1 may target GC regulatory genes that promote the Spt–GC reaction. Together, we identify a novel B cell–intrinsic mechanism of IFN-γR and STAT1 signaling that is central to Spt-GC development leading to autoimmunity. Because IFN-γR and STAT1 signaling are involved in SLE disease in both human and mouse models, targeting this pathway in Spt-GCs would be a promising treatment option for SLE disease.

MATERIALS AND METHODS

Mice. C57BL/6J (B6), B6.*Ifngr1$^{-/-}$* (B6.IFN-γR$_1$$^{-/-}$), B6.129S-*Stat1^{tm1Div}*/J (B6.*STAT1$^{-/-}$*), B6.129-*Stat1^{tm1Mam}*/ *Mmjax*(B6.*STAT1$^{fl/fl}$*),B6.Cd19$^{Cre/Cre}$,B6.129S7-*Rag1^{tm1Mom}*/ J (Rag$_1$$^{-/-}$), B6.129S2-*Ighm^{tm1Cgn}*/J (B6.μMT), B6.*Tbx21$^{-/-}$* (B6.*T-bet$^{-/-}$*), and B6.*Ifng$^{-/-}$* (B6.IFN-γ$^{-/-}$) mice were originally purchased from The Jackson Laboratory and bred in house. The development of B6 mice congenic for the *Sle1b* sublocus (named B6.*Sle1b*) and B6.HKIR mice were described previously (Wong et al., 2012). All animals were housed in the Pennsylvania State University Hershey Medical Center (PSUHMC) in a specific pathogen-free animal facility. All procedures were performed in accordance with the guidelines approved by the PSUHMC Institutional Animal Care and Use Committee.

Flow cytometry. Flow cytometric analysis of mouse splenocytes or BM cells was performed using the following Abs: Pacific blue–anti-B220 (RA3-6B2), Alexa Fluor 700–anti-CD4 (RM4-5), PE-anti–PD-1 (29F.1A12), Cy5–anti-CD86 (GL1), PeCy7–anti-CD95 (FAS, Jo2), PeCy7–anti-MHC II (M5/114.15.2), APC–anti-CD24 (HSA; M1/69), biotin–anti-Ly5.1 (BP-1; 6C3), FITC–anti-CD23 (B3B4), APC-anti–T-bet (4B10), APC-anti–IFN-γ (XMG1.2), and PE–Cy5-streptavidin (all purchased from BioLegend), as well as biotin–anti-CXCR5 (2G8), PE-anti–Bcl-6 (K112-91), and biotin–anti-CD119 (IFN-γR$_1$, GR20; purchased from BD). FITC–peanut agglutinin (PNA) was purchased from Vector Laboratories. PE–anti-IgM (eB121-15F9), APC–anti-CD93 (AA4.1), and FITC–anti–F4/80 (BM8) were purchased from eBioscience. The following Abs were used for phosphoflow analysis using a phosphoflow staining kit (BD): mouse anti-pSTAT1 (pY701; 4a), mouse anti-pSTAT1 (N terminus; 1/ Stat1), and mouse anti-pSTAT3 (pY705; 4/P-STAT3). For intracellular cytokines and transcription factor staining, cells were fixed and permeabilized using a cytoperm/cytofix kit (BD) and a FoxP3 staining buffer kit (eBioscience), respectively. Stained cells were analyzed using a flow cytometer (LSR II; BD). Data were acquired using FACSDiva software (BD) and analyzed using FlowJo software (Tree Star).

Immunohistochemistry. Immunohistochemical labeling of mouse spleen sections was performed using the following Abs and reagents. For immunofluorescence, PE–anti-CD4 (GK1.5), FITC-GL7, and APC–anti-IgD (11–26c.2a; all from BD) were used. For visible histology, HRP–PNA (Sigma-Aldrich) and anti-IgD-biotin (11–26; SouthernBiotech) were used. Biotinylated Abs were detected by streptavidin–alkaline phosphatase (Vector Laboratories). Ab binding was detected using a blue alkaline–phosphatase substrate kit and the NovaRed kit for peroxidase (both from Vector Laboratories). 5–6-µm spleen cryostat sections were prepared as previously described (Rahman et al., 2003).

Quantification of GC frequency and size by histology. Immunohistochemistry was performed using the aforementioned Abs. Images of stained spleen sections were captured using a fluorescence microscope (DM4000; Leica Biosystems) and Leica Biosystems software. GC area was measured using an area measurement tool (LASAF; Leica Biosystems). For GC frequency, total GC numbers were quantitated in five separate 10× field areas per spleen section in a blinded manner.

ELISPOT analysis. In brief, splenocytes in RPMI containing 10% FBS were plated at a concentration of 10^6 cells per well onto anti-IgM–, anti-IgG–, salmon sperm dsDNA– (Invitrogen), calf thymus histone– (Sigma-Aldrich), or nucleosome- (histone plated on a layer of dsDNA coating) coated multiscreen 96-well filtration plates (EMD Millipore). Serially diluted (1:2) cells were incubated for 6 h at 37°C. IgM-producing AFCs were detected using biotinylated anti–mouse IgM (Jackson ImmunoResearch Laboratories, Inc.) and streptavidin–alkaline phosphatase (Vector Laboratories). IgG-producing AFCs were detected using alkaline phosphatase–conjugated anti–mouse IgG (Molecular Probes). dsDNA-, histone-, and nucleosome-specific AFCs were detected by biotinylated anti-κ Abs (Invitrogen) followed by streptavidin–alkaline phosphatase (Vector Laboratories) or alkaline phosphatase–conjugated anti–mouse IgG (Molecular Probes). Plates were developed using a blue alkaline phosphatase substrate kit (III; Vector Laboratories). ELISPOTs were enumerated and analyzed using a computerized ELISPOT plate imaging/analysis system (Cellular Technology).

ELISA. For IgG or IgM detection, ELISA plates (Thermo Fisher Scientific) were coated with anti-IgM or anti-IgG (both from Invitrogen) capture Abs and detected using biotinylated anti–mouse IgM (Jackson ImmunoResearch Laboratories, Inc.) or alkaline phosphatase–conjugated anti–mouse IgG (Molecular Probes). Total IgG auto-Ab titers were measured in ELISA plates coated with salmon sperm dsDNA (Invitrogen), histone (Sigma-Aldrich), or nucleosome (histone plated on a layer of dsDNA coating) and detected with biotinylated anti-κ Abs (Invitrogen). IgG subtype–specific auto-Ab titers were detected by biotinylated IgG$_1$, biotinylated IgG$_{2b}$, and alkaline phosphatase IgG$_{2c}$ Abs (SouthernBio-

tech). Biotinylated Abs were detected by streptavidin–alkaline phosphatase (Vector Laboratories). The plates were developed by the PNPP (*p*-nitrophenyl phosphate, disodium salt; Thermo Fisher Scientific) substrates for alkaline phosphatase and read at 405 nm.

Immunizations. Mice were immunized i.p. with 200 µg/mouse NP-CGG (Biosearch Technologies) in imject alum (Thermo Fisher Scientific) followed by a booster immunization with 100 µg/mouse NP-CGG in alum 7 d later. Splenocytes were analyzed 14 d after initial immunization by flow cytometry.

Adoptive transfer. Magnetic-activated cell sorting (MACS)–purified T cells and B cells were mixed at a 3:1 ratio (B cells/T cells) and i.v. transferred into Rag$_1^{-/-}$ recipients. Recipients were analyzed after 2 mo for Spt-GC and Tfh cell development.

Generation of BM chimeric mice. 10–12-wk-old female B6.µMT (B6.Igh^{tm1Tim}) mice recipients were lethally irradiated with two doses of 450 rads of x rays (X-RAD 320iX Research Irradiator; Precision X-Ray) within a 4-h interval. Within 24 h of the second irradiation, each recipient i.v. received 10^7 T cell–depleted BM cells isolated from 8–10-wk-old female donor mice with 80% of cells from B6.µMT mice and 20% from B6 or B6.IFN-γR$_1^{-/-}$ mice. In a similar experiment, each B6.µMT recipient mouse i.v. received 10^7 T cell–depleted BM cells isolated from 8–10-wk-old female donor mice with 80% of cells from B6.µMT mice and 20% from B6.*Sle1b* or B6.*Sle1b*.IFN-γR$_1^{-/-}$ mice. Recipients were analyzed after 3 mo for Spt-GC and Tfh cell development.

DNA/RNA preparation for real-time RT-PCR. Total RNA from different populations of B cells (naive B cells, Spt-GC B cells, iGC B cells, and ex vivo–generated GC B cells) was isolated as described previously (Wong et al., 2015). In brief, total RNA was isolated using a TRIzol reagent (Thermo Fisher Scientific) according to the manufacturer's protocol. RT of the RNA was performed using a high-capacity RT kit (Applied Biosystems). Taqman PCR Master Mix kit or Power SYBR green PCR Master Mix kits were used to quantify gene expression (Applied Biosystems) using a real-time PCR system (StepOne Plus; Applied Biosystems). Primers for the *bcl-6*, *Ifng*, and *tbx21* genes were synthesized by IDT Technologies. Primer sequences were as follows: *Bcl-6*, forward (5′-CTAGCGTCTGACCAGGATCCA-3′) and reverse (5′-AGGTCACGCTCAAGGTTTGC-3′); *Ifng*, forward (5′-CGGCACAGTCATTGAAAGCC-3′) and reverse (5′-TGCATCCTTTTTCGCCTTGC-3′); *Tbx21*, forward (5′-GCCAGGGAACCGCTTATATG-3′) and reverse (5′-GACGATCATCTGGGTCACATTGT-3′); and actin (*Actb*), which was used as the reference gene for sample normalization, forward (5′-ATGTGGATCAGCAAGCGGGA-3′) and reverse (5′-AAGGGTGTAAAACGAAGCTCA-3′). cDNA was amplified under the following conditions for all primer sets: one

cycle at 95°C for 10 min followed by 40 cycles at 95°C for 15 s and 60°C for 1 min.

In vitro B cell isolation, culture, and stimulation. Isolated splenocytes were cultured in RPMI 1640 (Gibco) containing 10% FBS. To assay for cytokine production, splenocytes were cultured in GolgiStop (BD) and stimulated with phorbol 12-myristate 13-acetate (PMA) and ionomycin for 4 h at 37°C and 5% CO_2. After stimulation, B cells were processed for intracellular cytokine staining as described in the Flow cytometry section.

In vitro GC B cell development assay. Ex vivo GC B cells were generated according to a protocol described previously (Nojima et al., 2011). In brief, 5×10^5 MACS-purified naive B cells (Miltenyi Biotec) were cultured in a 6-well plate (BD) over an adherent layer of $3–4 \times 10^6$ γ-irradiated (120 Gy) 40LB fibroblast cells. 40LB fibroblasts express CD40L and BAFF to stimulate B cell differentiation in the presence of IL-4. The culture media contained RPMI 1640 medium (Corning) supplemented with 10% FCS, β-ME (5.5×10^{-5} M), 10 mM Hepes, 1 mM sodium pyruvate, 100 U/ml penicillin, 100 µg/ml streptomycin (Gibco), and 5 ng/ml rIL-4 (PeproTech). On the fourth day of culture, cells were harvested, washed, and analyzed for surface marker expression to confirm GC B cell phenotype and plated on another feeder layer of fibroblasts supplemented with media alone, rIL-4, or 10 ng/ml rIFN-γ (PeproTech) for another 4 d. On the eighth day of culture, cells were harvested and analyzed for surface marker expression by flow cytometry or processed for RNA preparation.

Phosphoflow analysis. For pSTAT kinetics experiments, MACS-purified B cells were activated with 5 µg/ml anti-IgM (Jackson ImmunoResearch Laboratories, Inc.) and/or 10 ng/ml rIFN-γ (PeproTech) for the indicated time intervals at 37°C. After activation, cells were fixed with a lyse/fix buffer (BD) for 10 min at 37°C. Cells were permeabilized with a perm/wash buffer (BD) for 30 min at room temperature. After two washes with a perm/wash buffer, cells were stained with anti-B220 and phosphoflow Abs (described in the Materials and methods section Flow cytometry; BD) for 1 h at 4°C. For analysis of STAT staining in GC B cells, total splenocytes were fixed, permeabilized, and stained with anti-B220, anti-PNA, anti-CD95, and phosphoflow Abs.

HEp-2 ANA detection. For the detection of ANA seropositivity, sera from mice were incubated at a 1:50 dilution in PBS on HEp-2 ANA detection slides (Antibodies Inc.) and detected with FITC–rat anti-κ (H139-52.1; SouthernBiotech).

Kidney histopathology. Kidneys from 6-mo-old females were fixed in 10% neutral buffered formalin and embedded in paraffin. Kidney sections were cut at 3-µm thickness and periodic acid–Schiff stained. Pathology scores were obtained with a microscope (BX51; Olympus) and cellSens standard 1.12 imaging software (Olympus). A veterinary pathologist blinded

to the genotype of the mice evaluated one kidney section per mouse. Each individual glomerulus was examined at 400× magnification and scored from 0 (normal) to 4 (severe) based on glomerular size and lobulation, presence of karyorrhectic nuclear debris, capillary basement membrane thickening, and the degree of mesangial matrix expansion/proliferation.

Statistical analysis. Comparisons of two groups were analyzed using an unpaired, nonparametric, Mann–Whitney Student's t test. One-way ANOVA, with a follow-up Tukey multiple-comparison test, was used to compare more than two groups. Prism 6 (GraphPad Software) was used for all analyses. Wherever indicated, p-values are as follows: *, $P < 0.05$; **, $P < 0.01$; ***, $P < 0.001$; ****, $P < 0.001$. Bars reflect mean values, and error bars reflect standard deviation of the mean unless indicated otherwise.

REFERENCES

Allman, D., R.C. Lindsley, W. DeMuth, K. Rudd, S.A. Shinton, and R.R. Hardy. 2001. Resolution of three nonproliferative immature splenic B cell subsets reveals multiple selection points during peripheral B cell maturation. *J. Immunol.* 167:6834–6840. http://dx.doi.org/10.4049/jimmunol.167.12.6834

Avery, D.T., E.K. Deenick, C.S. Ma, S. Suryani, N. Simpson, G.Y. Chew, T.D. Chan, U. Palendira, J. Bustamante, S. Boisson-Dupuis, et al. 2010. B cell–intrinsic signaling through IL-21 receptor and STAT3 is required for establishing long-lived antibody responses in humans. *J. Exp. Med.* 207:155–171. http://dx.doi.org/10.1084/jem.20091706

Balomenos, D., R. Rumold, and A.N. Theofilopoulos. 1998. Interferon-gamma is required for lupus-like disease and lymphoaccumulation in MRL-lpr mice. *J. Clin. Invest.* 101:364–371. http://dx.doi.org/10.1172/JCI750

Berland, R., L. Fernandez, E. Kari, J.H. Han, I. Lomakin, S. Akira, H.H. Wortis, J.F. Kearney, A.A. Ucci, and T. Imanishi-Kari. 2006. Toll-like receptor 7-dependent loss of B cell tolerance in pathogenic autoantibody knockin mice. *Immunity.* 25:429–440. http://dx.doi.org/10.1016/j.immuni.2006.07.014

Bessa, J., M. Kopf, and M.F. Bachmann. 2010. Cutting edge: IL-21 and TLR signaling regulate germinal center responses in a B cell–intrinsic manner. *J. Immunol.* 184:4615–4619. http://dx.doi.org/10.4049/jimmunol.0903949

Cappione, A. III, J.H. Anolik, A. Pugh-Bernard, J. Barnard, P. Dutcher, G. Silverman, and I. Sanz. 2005. Germinal center exclusion of autoreactive B cells is defective in human systemic lupus erythematosus. *J. Clin. Invest.* 115:3205–3216. http://dx.doi.org/10.1172/JCI24179

Caron, G., D. Duluc, I. Frémaux, P. Jeannin, C. David, H. Gascan, and Y. Delneste. 2005. Direct stimulation of human T cells via TLR5 and TLR7/8: flagellin and R-848 up-regulate proliferation and IFN-γ production by memory CD4^{+} T cells. *J. Immunol.* 175:1551–1557. http://dx.doi.org/10.4049/jimmunol.175.3.1551

Chalifour, A., P. Jeannin, J.F. Gauchat, A. Blaecke, M. Malissard, T. N'Guyen, N. Thieblemont, and Y. Delneste. 2004. Direct bacterial protein PAMP recognition by human NK cells involves TLRs and triggers α-defensin production. *Blood*. 104:1778–1783. http://dx.doi.org/10.1182/blood-2003-08-2820

Csiszár, A., G. Nagy, P. Gergely, T. Pozsonyi, and E. Pócsik. 2000. Increased interferon-γ (IFN-γ), IL-10 and decreased IL-4 mRNA expression in peripheral blood mononuclear cells (PBMC) from patients with systemic lupus erythematosus (SLE). *Clin. Exp. Immunol.* 122:464–470. http://dx.doi.org/10.1046/j.1365-2249.2000.01369.x

Dai, X., R.G. James, T. Habib, S. Singh, S. Jackson, S. Khim, R.T. Moon, D. Liggitt, A. Wolf-Yadlin, J.H. Buckner, and D.J. Rawlings. 2013. A disease-associated PTPN22 variant promotes systemic autoimmunity in murine models. *J. Clin. Invest.* 123:2024–2036. http://dx.doi.org/10.1172/JCI66963

Diamond, B., J.B. Katz, E. Paul, C. Aranow, D. Lustgarten, and M.D. Scharff. 1992. The role of somatic mutation in the pathogenic anti-DNA response. *Annu. Rev. Immunol.* 10:731–757. http://dx.doi.org/10.1146/annurev.iy.10.040192.003503

Dong, J., Q.X. Wang, C.Y. Zhou, X.F. Ma, and Y.C. Zhang. 2007. Activation of the STAT1 signalling pathway in lupus nephritis in MRL/lpr mice. *Lupus*. 16:101–109. http://dx.doi.org/10.1177/0961203306075383

Fornek, J.L., L.T. Tygrett, T.J. Waldschmidt, V. Poli, R.C. Rickert, and G.S. Kansas. 2006. Critical role for Stat3 in T-dependent terminal differentiation of IgG B cells. *Blood*. 107:1085–1091. http://dx.doi.org/10.1182/blood-2005-07-2871

Haas, C., B. Ryffel, and M. Le Hir. 1998. IFN-γ receptor deletion prevents autoantibody production and glomerulonephritis in lupus-prone (NZB x NZW)F1 mice. *J. Immunol.* 160:3713–3718.

Hardy, R.R., C.E. Carmack, S.A. Shinton, J.D. Kemp, and K. Hayakawa. 1991. Resolution and characterization of pro-B and pre-pro-B cell stages in normal mouse bone marrow. *J. Exp. Med.* 173:1213–1225. http://dx.doi.org/10.1084/jem.173.5.1213

Harigai, M., M. Kawamoto, M. Hara, T. Kubota, N. Kamatani, and N. Miyasaka. 2008. Excessive production of IFN-γ in patients with systemic lupus erythematosus and its contribution to induction of B lymphocyte stimulator/B cell-activating factor/TNF ligand superfamily-13B. *J. Immunol.* 181:2211–2219. http://dx.doi.org/10.4049/jimmunol.181.3.2211

Harris, D.P., L. Haynes, P.C. Sayles, D.K. Duso, S.M. Eaton, N.M. Lepak, L.L. Johnson, S.L. Swain, and F.E. Lund. 2000. Reciprocal regulation of polarized cytokine production by effector B and T cells. *Nat. Immunol.* 1:475–482. http://dx.doi.org/10.1038/82717

Harris, D.P., S. Goodrich, A.J. Gerth, S.L. Peng, and F.E. Lund. 2005. Regulation of IFN-γ production by B effector 1 cells: essential roles for T-bet and the IFN-γ receptor. *J. Immunol.* 174:6781–6790. http://dx.doi.org/10.4049/jimmunol.174.11.6781

Hua, Z., A.J. Gross, C. Lamagna, N. Ramos-Hernández, P. Scapini, M. Ji, H. Shao, C.A. Lowell, B. Hou, and A.L. DeFranco. 2014. Requirement for MyD88 signaling in B cells and dendritic cells for germinal center anti-nuclear antibody production in Lyn-deficient mice. *J. Immunol.* 192:875–885. http://dx.doi.org/10.4049/jimmunol.1300683

Jackson, S.W., N.E. Scharping, N.S. Kolhatkar, S. Khim, M.A. Schwartz, Q.Z. Li, K.L. Hudkins, C.E. Alpers, D. Liggitt, and D.J. Rawlings. 2014. Opposing impact of B cell-intrinsic TLR7 and TLR9 signals on autoantibody repertoire and systemic inflammation. *J. Immunol.* 192:4525–4532. http://dx.doi.org/10.4049/jimmunol.1400098

Jackson, S.W., N.S. Kolhatkar, and D.J. Rawlings. 2015. B cells take the front seat: dysregulated B cell signals orchestrate loss of tolerance and

autoantibody production. *Curr. Opin. Immunol.* 33:70–77. http://dx.doi.org/10.1016/j.coi.2015.01.018

Jacob, C.O., P.H. van der Meide, and H.O. McDevitt. 1987. In vivo treatment of (NZB X NZW)F1 lupus-like nephritis with monoclonal antibody to gamma interferon. *J. Exp. Med.* 166:798–803. http://dx.doi.org/10.1084/jem.166.3.798

Johnson, L.M., and P. Scott. 2007. STAT1 expression in dendritic cells, but not T cells, is required for immunity to *Leishmania major*. *J. Immunol.* 178:7259–7266. http://dx.doi.org/10.4049/jimmunol.178.11.7259

Kim, K., S.K. Cho, A. Sestak, B. Namjou, C. Kang, and S.C. Bae. 2010. Interferon-gamma gene polymorphisms associated with susceptibility to systemic lupus erythematosus. *Ann. Rheum. Dis.* 69:1247–1250. http://dx.doi.org/10.1136/ard.2009.117572

Kim, S.J., Y.R. Zou, J. Goldstein, B. Reizis, and B. Diamond. 2011. Tolerogenic function of Blimp-1 in dendritic cells. *J. Exp. Med.* 208:2193–2199. http://dx.doi.org/10.1084/jem.20110658

Lawson, B.R., G.J. Prud'homme, Y. Chang, H.A. Gardner, J. Kuan, D.H. Kono, and A.N. Theofilopoulos. 2000. Treatment of murine lupus with cDNA encoding IFN-γR/Fc. *J. Clin. Invest.* 106:207–215. http://dx.doi.org/10.1172/JCI10167

Leadbetter, E.A., I.R. Rifkin, A.M. Hohlbaum, B.C. Beaudette, M.J. Shlomchik, and A. Marshak-Rothstein. 2002. Chromatin-IgG complexes activate B cells by dual engagement of IgM and toll-like receptors. *Nature*. 416:603–607. http://dx.doi.org/10.1038/416603a

Lee, S.K., D.G. Silva, J.L. Martin, A. Pratama, X. Hu, P.P. Chang, G. Walters, and C.G. Vinuesa. 2012. Interferon-γ excess leads to pathogenic accumulation of follicular helper T cells and germinal centers. *Immunity*. 37:880–892. http://dx.doi.org/10.1016/j.immuni.2012.10.010

Linterman, M.A., L. Beaton, D. Yu, R.R. Ramiscal, M. Srivastava, J.J. Hogan, N.K. Verma, M.J. Smyth, R.J. Rigby, and C.G. Vinuesa. 2010. IL-21 acts directly on B cells to regulate Bcl-6 expression and germinal center responses. *J. Exp. Med.* 207:353–363. http://dx.doi.org/10.1084/jem.20091738

Lu, X., E.E. Zoller, M.T. Weirauch, Z. Wu, B. Namjou, A.H. Williams, J.T. Ziegler, M.E. Comeau, M.C. Marion, S.B. Glenn, et al. 2015. Lupus risk variant increases pSTAT1 binding and decreases ETS1 expression. *Am. J. Hum. Genet.* 96:731–739. http://dx.doi.org/10.1016/j.ajhg.2015.03.002

Luzina, I.G., S.P. Atamas, C.E. Storrer, L.C. daSilva, G. Kelsoe, J.C. Papadimitriou, and B.S. Handwerger. 2001. Spontaneous formation of germinal centers in autoimmune mice. *J. Leukoc. Biol.* 70:578–584.

Nojima, T., K. Haniuda, T. Moutai, M. Matsudaira, S. Mizokawa, I. Shiratori, T. Azuma, and D. Kitamura. 2011. *In-vitro* derived germinal centre B cells differentially generate memory B or plasma cells *in vivo*. *Nat. Commun.* 2:465. http://dx.doi.org/10.1038/ncomms1475

Nutt, S.L., and D.M. Tarlinton. 2011. Germinal center B and follicular helper T cells: siblings, cousins or just good friends? *Nat. Immunol.* 12:472–477. http://dx.doi.org/10.1038/ni.2019

Ozmen, L., D. Roman, M. Fountoulakis, G. Schmid, B. Ryffel, and G. Garotta. 1995. Experimental therapy of systemic lupus erythematosus: the treatment of NZB/W mice with mouse soluble interferon-γ receptor inhibits the onset of glomerulonephritis. *Eur. J. Immunol.* 25:6–12. http://dx.doi.org/10.1002/eji.1830250103

Peng, S.L., S.J. Szabo, and L.H. Glimcher. 2002. T-bet regulates IgG class switching and pathogenic autoantibody production. *Proc. Natl. Acad. Sci. USA*. 99:5545–5550. http://dx.doi.org/10.1073/pnas.082114899

Pollard, K.M., D.M. Cauvi, C.B. Toomey, K.V. Morris, and D.H. Kono. 2013. Interferon-γ and systemic autoimmunity. *Discov. Med.* 16:123–131.

Rahman, Z.S. 2011. Impaired clearance of apoptotic cells in germinal centers: implications for loss of B cell tolerance and induction of autoimmunity. *Immunol. Res.* 51:125–133. http://dx.doi.org/10.1007/s12026-011-8248-4

Rahman, Z.S., S.P. Rao, S.L. Kalled, and T. Manser. 2003. Normal induction but attenuated progression of germinal center responses in BAFF and

BAFF–R signaling-deficient mice. *J. Exp. Med.* 198:1157–1169. http://dx.doi.org/10.1084/jem.20030495

Rahman, Z.S., B. Alabyev, and T. Manser. 2007. FcγRIIB regulates autoreactive primary antibody–forming cell, but not germinal center B cell, activity. *J. Immunol.* 178:897–907. http://dx.doi.org/10.4049/jimmunol.178.2.897

Ramana, C.V., M.P. Gil, R.D. Schreiber, and G.R. Stark. 2002. Stat1-dependent and –independent pathways in IFN-γ-dependent signaling. *Trends Immunol.* 23:96–101. http://dx.doi.org/10.1016/S1471-4906(01)02118-4

Rankin, A.L., H. Guay, D. Herber, S.A. Bertino, T.A. Duzanski, Y. Carrier, S. Keegan, M. Senices, N. Stedman, M. Ryan, et al. 2012. IL-21 receptor is required for the systemic accumulation of activated B and T lymphocytes in MRL/MpJ-Fas*lpr/lpr*/J mice. *J. Immunol.* 188:1656–1667. http://dx.doi.org/10.4049/jimmunol.1003871

Rubtsov, A.V., K. Rubtsova, J.W. Kappler, and P. Marrack. 2013. TLR7 drives accumulation of ABCs and autoantibody production in autoimmune-prone mice. *Immunol. Res.* 55:210–216. http://dx.doi.org/10.1007/s12026-012-8365-8

Rubtsova, K., A.V. Rubtsov, L.F. van Dyk, J.W. Kappler, and P. Marrack. 2013. T-box transcription factor T-bet, a key player in a unique type of B-cell activation essential for effective viral clearance. *Proc. Natl. Acad. Sci. USA.* 110:E3216–E3224. http://dx.doi.org/10.1073/pnas.1312348110

Rubtsova, K., A.V. Rubtsov, M.P. Cancro, and P. Marrack. 2015. Age-associated B cells: a T-bet-dependent effector with roles in protective and pathogenic immunity. *J. Immunol.* 195:1933–1937. http://dx.doi.org/10.4049/jimmunol.1501209

Sanz, I. 2014. Rationale for B cell targeting in SLE. *Semin. Immunopathol.* 36:365–375. http://dx.doi.org/10.1007/s00281-014-0430-z

Sato, T., C. Selleri, N.S. Young, and J.P. Maciejewski. 1997. Inhibition of interferon regulatory factor-1 expression results in predominance of cell growth stimulatory effects of interferon-γ due to phosphorylation of Stat1 and Stat3. *Blood.* 90:4749–4758.

Schwarting, A., T. Wada, K. Kinoshita, G. Tesch, and V.R. Kelley. 1998. IFN-γ receptor signaling is essential for the initiation, acceleration, and destruction of autoimmune kidney disease in MRL-*Fas*lpr mice. *J. Immunol.* 161:494–503.

Soni, C., E.B. Wong, P.P. Domeier, T.N. Khan, T. Satoh, S. Akira, and Z.S. Rahman. 2014. B cell-intrinsic TLR7 signaling is essential for the development of spontaneous germinal centers. *J. Immunol.* 193:4400–4414. http://dx.doi.org/10.4049/jimmunol.1401720

Su, L., R.C. Rickert, and M. David. 1999. Rapid STAT phosphorylation via the B cell receptor. Modulatory role of CD19. *J. Biol. Chem.* 274:31770–31774. http://dx.doi.org/10.1074/jbc.274.45.31770

Tellier, J., and S.L. Nutt. 2013. The unique features of follicular T cell subsets. *Cell. Mol. Life Sci.* 70:4771–4784. http://dx.doi.org/10.1007/s00018-013-1420-3

Thibault, D.L., A.D. Chu, K.L. Graham, I. Balboni, L.Y. Lee, C. Kohlmoos, A. Landrigan, J.P. Higgins, R. Tibshirani, and P.J. Utz. 2008. IRF9 and STAT1 are required for IgG autoantibody production and B cell expression of TLR7 in mice. *J. Clin. Invest.* 118:1417–1426. http://dx.doi.org/10.1172/JCI30065

Tiller, T., J. Kofer, C. Kreschel, C.E. Busse, S. Riebel, S. Wickert, F. Oden, M.M. Mertes, M. Ehlers, and H. Wardemann. 2010. Development of

self-reactive germinal center B cells and plasma cells in autoimmune FcγRIIB–deficient mice. *J. Exp. Med.* 207:2767–2778. http://dx.doi.org/10.1084/jem.20100171

Viglianti, G.A., C.M. Lau, T.M. Hanley, B.A. Miko, M.J. Shlomchik, and A. Marshak-Rothstein. 2003. Activation of autoreactive B cells by CpG dsDNA. *Immunity.* 19:837–847. http://dx.doi.org/10.1016/S1074-7613(03)00323-6

Vinuesa, C.G., I. Sanz, and M.C. Cook. 2009. Dysregulation of germinal centres in autoimmune disease. *Nat. Rev. Immunol.* 9:845–857. http://dx.doi.org/10.1038/nri2637

Vuyyuru, R., C. Mohan, T. Manser, and Z.S. Rahman. 2009. The lupus susceptibility locus Sle1 breaches peripheral B cell tolerance at the antibody-forming cell and germinal center checkpoints. *J. Immunol.* 183:5716–5727. http://dx.doi.org/10.4049/jimmunol.0804215

Walsh, E.R., P. Pisitkun, E. Voynova, J.A. Deane, B.L. Scott, R.R. Caspi, and S. Bolland. 2012. Dual signaling by innate and adaptive immune receptors is required for TLR7-induced B-cell–mediated autoimmunity. *Proc. Natl. Acad. Sci. USA.* 109:16276–16281. http://dx.doi.org/10.1073/pnas.1209372109

Wandstrat, A.E., C. Nguyen, N. Limaye, A.Y. Chan, S. Subramanian, X.H. Tian, Y.S. Yim, A. Pertsemlidis, H.R. Garner Jr., L. Morel, and E.K. Wakeland. 2004. Association of extensive polymorphisms in the SLAM/CD2 gene cluster with murine lupus. *Immunity.* 21:769–780. http://dx.doi.org/10.1016/j.immuni.2004.10.009

Welcher, A.A., M. Boedigheimer, A.J. Kivitz, Z. Amoura, J. Buyon, A. Rudinskaya, K. Latinis, K. Chiu, K.S. Oliner, M.A. Damore, et al. 2015. Blockade of interferon-γ normalizes interferon-regulated gene expression and serum CXCL10 levels in patients with systemic lupus erythematosus. *Arthritis Rheumatol.* 67:2713–2722. http://dx.doi.org/10.1002/art.39248

Wellmann, U., M. Letz, M. Herrmann, S. Angermüller, J.R. Kalden, and T.H. Winkler. 2005. The evolution of human anti-double-stranded DNA autoantibodies. *Proc. Natl. Acad. Sci. USA.* 102:9258–9263. http://dx.doi.org/10.1073/pnas.0500132102

Wong, E.B., T.N. Khan, C. Mohan, and Z.S. Rahman. 2012. The lupus-prone NZM2410/NZW strain–derived *Sle1b* sublocus alters the germinal center checkpoint in female mice in a B cell–intrinsic manner. *J. Immunol.* 189:5667–5681. http://dx.doi.org/10.4049/jimmunol.1201661

Wong, E.B., C. Soni, A.Y. Chan, P.P. Domeier, T. Shwetank, T. Abraham, N. Limaye, T.N. Khan, M.J. Elias, S.B. Chodisetti, et al. 2015. B cell-intrinsic CD84 and Ly108 maintain germinal center B cell tolerance. *J. Immunol.* 194:4130–4143. http://dx.doi.org/10.4049/jimmunol.1403023

Xu, W., and J.J. Zhang. 2005. Stat1-dependent synergistic activation of T-bet for IgG2a production during early stage of B cell activation. *J. Immunol.* 175:7419–7424. http://dx.doi.org/10.4049/jimmunol.175.11.7419

Zotos, D., J.M. Coquet, Y. Zhang, A. Light, K. D'Costa, A. Kallies, L.M. Corcoran, D.I. Godfrey, K.M. Toellner, M.J. Smyth, et al. 2010. IL-21 regulates germinal center B cell differentiation and proliferation through a B cell–intrinsic mechanism. *J. Exp. Med.* 207:365–378. http://dx.doi.org/10.1084/jem.20091777